HHS Public Access

Author manuscript

J Comp Neurol. Author manuscript; available in PMC 2017 December 15.

Published in final edited form as:

J Comp Neurol. 2016 December 15; 524(18): 3729–3746. doi:10.1002/cne.24027.

Prolonged corticosterone exposure induces dendritic spine remodeling and attrition in the rat medial prefrontal cortex

Rachel M. Anderson, **Ryan M. Glanz**, **Shane B. Johnson**, **Mary M. Miller**, **Sara Romig-Martin**, and **Jason J. Radley**

Department of Psychological and Brain Sciences and Program in Neuroscience, University of Iowa, Iowa City, IA 52242

Abstract

The stress-responsive hypothalamo-pituitary-adrenal (HPA) axis plays a central role in promoting adaptations acutely, while adverse effects on physiology and behavior following chronic challenges may result from over-activity of this system. Elevations in glucocorticoids, the end-products of HPA activation, play roles in adaptive and maladaptive processes by targeting cognate receptors throughout neurons in limbic cortical networks to alter synaptic functioning. Since previous work has shown that chronic stress leads to functionally relevant regressive alterations in dendritic spine shape and number in pyramidal neurons in medial prefrontal cortex (mPFC), here we examine the capacity of sustained increases in circulating corticosterone alone to alter dendritic spine morphology and density in this region. Rats were implanted with subcutaneous corticosterone pellets to provide continuous exposure to levels approximating the circadian mean or peak of the steroid for 1, 2, or 3 weeks. Pyramidal neurons in prelimbic area of mPFC were selected for intracellular fluorescent dye-filling, followed by high-resolution 3D imaging and analysis of dendritic arborization and spine morphometry. Two or more weeks of corticosterone exposure decreased dendritic spine volume in mPFC, whereas higher dose exposure of the steroid resulted in apical dendritic retraction and spine loss in the same cell population, with thin spine subtypes showing the greatest degree of attrition. Finally, these structural alterations were noted to persist following a 3-week washout period and corresponding restoration of circadian HPA rhythmicity. These studies suggest that prolonged disruptions in adrenocortical functioning may be sufficient to induce enduring regressive structural and functional alterations in mPFC.

Graphical abstract

Using high-resolution confocal laser-scanning microscopy, the authors show that prolonged elevations in corticosterone induce persistent alterations in dendritic spine morphology and decreased density in rat medial prefrontal cortex. This darkfield image shows layer 2/3 prefrontal pyramidal neurons selected for intracellular dye-filling with Lucifer Yellow (cyan).

Correspondence: Dr. Jason Radley, Department of Psychology, University of Iowa, E232 Seashore Hall, Iowa City, IA 52242. Tel. 319-353-0152; Jason-radley@uiowa.edu.

Author contributions: R.M.A. and J.J.R. designed research; R.M.A., R.M.G., S.B.J., M.M.M., S.R.M., and J.J.R performed research; R.M.A., R.M.G, and J.J.R. analyzed data; R.M.A. and J.J.R wrote the paper

The authors declare no competing financial interests.

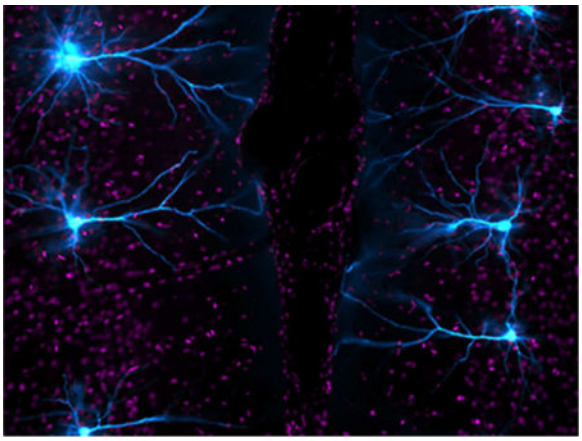

Keywords

glucocorticoids; HPA axis; prelimbic; confocal laser-scanning microscopy; NeuronStudio

INTRODUCTION

A hallmark of the mammalian stress response entails activation of the hypothalamo-pituitary-adrenal (HPA) axis – a neuroendocrine cascade that stimulates glucocorticoid secretion from the adrenal gland (Antoni, 1986). A substantial body of research suggests that the capacity of environmentally salient stimuli to activate the HPA axis depends upon modulatory control from a network of limbic forebrain cell groups that coordinate physiological and behavioral responses for adaptive coping (Feldman and Conforti, 1980; Diorio et al., 1993; Herman et al., 1995; Jaferi and Bhatnagar, 2006). In rodents, the medial prefrontal cortex (mPFC) is exemplary in this regard, performing both cognitive operations important for behavioral adaptation and neuroendocrine adjustments under stressful conditions. The prelimbic area (PL) is a centrally-located subfield within mPFC that straddles two broad functional domains, with more dorsal- and ventral-lying regions issuing projections that access distinct neural circuitries to modulate limbic-cognitive and visceromotor functions, respectively (Sesack et al., 1989; Vertes, 2004; Gabbott et al., 2005). PL exhibits robust structural and functional plasticity in response to a variety of environmental stimuli and experiences, thus increasing its repertoire of response capabilities under changing contexts such as chronic stress. Whereas glucocorticoids have widespread effects on prefrontal functions relevant for adaptation during acute challenges (Shors et al., 1992; McIntyre et al., 2003; Yuen et al., 2009), perturbations in HPA activity following prolonged stress are associated with maladaptive changes in many of these responses (Mizoguchi et al., 2000; Hains et al., 2009; Hinwood et al., 2012; McKlveen et al., 2013; Radley et al., 2013).

Evidence from our laboratory and others has shown that chronic stress is associated with structural remodeling of dendritic spines in mPFC pyramidal neurons and accompanying impairments in cognitive functioning (Liston et al., 2006; Radley et al., 2006; Radley et al., 2008; Radley et al., 2013), suggesting a role for altered adrenocortical activity in producing

these changes. Whereas there is an extensive literature highlighting the capacity of glucocorticoids to alter hippocampal (Watanabe et al., 1992a; Watanabe et al., 1992b; McEwen, 1998; Sousa et al., 2000; Alfarez et al., 2009; Morales-Medina et al., 2009; Tanokashira et al., 2012; Wosiski-Kuhn et al., 2014) and amygdala plasticity (Vyas et al., 2002; Mitra et al., 2005; Vyas et al., 2006; Mitra and Sapolsky, 2008; Grillo et al., 2015), information regarding glucocorticoid effects on structural plasticity in mPFC has not been as forthcoming. Evidence that prolonged elevations in glucocorticoids induce regressive dendritic spine alterations in mPFC (Liu and Aghajanian, 2008; Gourley et al., 2013), and in related cortical areas (Liston and Gan, 2011; Liston et al., 2013), are contrasted by conflicting reports of either no change (Cerqueira et al., 2007), or even increased dendritic spine density in mPFC (Seib and Wellman, 2003). Another complicating factor in evaluating the available evidence is that much of it is derived from Golgi-based approaches that hamper visualization of small spines that comprise ~50% of the total population (e.g., see Dumitriu et al., 2011). To this end, we critically examined the effects of continuous corticosterone (B) exposure on rat dendritic spine density and morphometric alterations in pyramidal neurons in PL using a high-resolution 3-D analytic approach (Rodriguez et al., 2006; Radley et al., 2008). We found that continuous B exposure for at least two weeks induced enduring dendritic spine remodeling and loss in PL, that persisted even after 3 weeks of restoration of normal HPA axis rhythmicity. These studies highlight a prominent role for alterations in mPFC that may result from repeated stress exposure or other contexts, such as Cushing's syndrome or aging.

MATERIALS AND METHODS

Animals

The animals used in this study were 3-month-old male Sprague Dawley albino rats (Charles River Laboratories). Rats were single-housed and maintained on a 12:12 h light/dark cycle (lights on at 0600), with free access to food and water. All experimental protocols were approved by the Institutional Animal Care and Use Committee of the University of Iowa.

Glucocorticoid treatment regimens

Experiment 1: Effects of varying doses of B on structural plasticity in PL—Rats were adrenalectomized and implanted with slow-release B pellets (i.e., 100 and 200 mg) to clamp circulating levels of this hormone to that of either the circadian mean (~9 μg/dl) or peak (~14 μg/dl; see Results) over a 2-week period for the assessment of structural plasticity effects in PL neurons. The decision to perform adrenalectomies in groups of rats receiving constant B was based upon the desire to provide an independent assessment of B pellet efficacy that may otherwise be masked by endogenous adrenocortical activity in an intact animal. Rats were anesthetized with isoflurane and adrenalectomized by the dorsal approach. In the same surgical procedure, adrenalectomized rats were implanted subcutaneously in the interscapular region with 100 mg (N = 9) or 200 mg (N = 15) B pellets that provide a constant and slow release into the general circulation for 3 weeks (Innovative Research of America, Sarasota, Florida). An additional group of rats received a sham adrenalectomy (N = 21), which involved all of the same procedural steps absent removal of the adrenal gland, and were then implanted with inert cholesterol pellets of equal

weight as the B pellets. On day 14, B pellet efficacy and baseline adrenocortical activity in B-replaced and sham rats, respectively, were confirmed by collection of repeated blood samples at AM and PM times and radioimmunoassay of B, and all rats were perfused on the morning of day 15.

Experiment 2: Persistence of B-induced structural alterations in PL following a 3-week recovery period—To assess the persistence of glucocorticoid-induced alterations in PL neuronal architecture, this experiment involved replacement with high dose B pellets (200 mg) spanning the 3-week duration of its release capability, followed by a 3-week recovery period (N = 14). Rats in these experiments were not adrenalectomized in order to allow for the normalization of circadian HPA activity through the course of the 3-week recovery period. A second group of rats received the same treatment course of B (N = 12), however their pellet implants were staggered to begin during the second 3-week period of the experiment, in order for the perfusion and cell loading procedures to be phase-locked with the B + recovery group. A third group of rats received implantation of sham cholesterol pellets (N = 10), randomized between the first and second 3-week interval to parallel procedures in the two groups of B-treated rats. On days 14 and 35, rats from all three groups were subjected to repeated AM and PM blood sampling for radioimmunoassay of plasma B levels. Pellet efficacy (on day 14) and normalization of HPA activity (on day 35) were assessed in the B/recovery group, whereas B efficacy and baseline adrenocortical activity were confirmed in B- and sham-implanted rats (day 35 and 14 respectively).

Experiment 3: Effects of short-term B exposure on structural plasticity in PL—To acquire information regarding the temporal characteristics of glucocorticoid-induced alterations in PL, dendritic spine morphology was examined in rats exposed to high dose B (200 mg) as compared with sham-implanted controls for 7 days (N = 12/group). B pellet efficacy and baseline adrenocortical activity in B-replaced and sham rats were confirmed by collection of repeated blood samples at AM and PM times and radioimmunoassay of B on day 5 of steroid exposure.

Blood collection and radioimmunoassay

Adrenocortical activity was assessed by obtaining blood from the tail vein of rats at 0700 and 1700 h of the day of sampling. Previous work from our laboratory has shown that these time points of sampling correspond well with nadir AM and peak PM values of B secretory activity in adrenally-intact rats. For blood collection, rats were restrained briefly (15–30 s), and a small longitudinal incision was made at the distal tip of the tail with a sterile blade. Blood samples (~200 μl) were collected into chilled plastic microfuge tubes containing EDTA and aprotinin, centrifuged, and fractionated for storage of plasma at −80°C until assayed. Plasma B was measured without extraction, using an antiserum raised in rabbits against a B-BSA conjugate, and ^{125}I-B-BSA as tracer (MP Biomedicals). Assay sensitivity was 0.8 μg/dl; intra- and interassay coefficients of variance were 5% and 10%, respectively.

Histology and tissue processing

Rats were anesthetized with sodium pentobarbital (100 mg/kg, i.p.) and perfused via the ascending aorta with 100 ml 1% PFA and 0.125% glutaraldehyde in 0.1 M phosphate

buffered saline (PBS, pH 7.4) followed by 500 ml of 4% PFA and 0.125% glutaraldehyde in PBS, at a flow rate of 55 ml/min. After post-fixation, the pregenual pole of the cortex was sectioned coronally into 250-μm-thick slabs using an oscillating tissue slicer (VT-1000S, Leica) and stored in 0.1 M PBS containing 0.1% sodium azide at 4°C until the time of cell loading.

Intracellular dye injections

The procedures used in this experiment are based on previous reports using the same methodology (Radley et al., 2006; Anderson et al., 2014). Coronal tissue slabs were treated in the DNA-binding fluorescent stain 4′,6-diamidino-2-phenylindole (DAPI, Invitrogen) to distinguish between nuclear lamination patterns that distinguish PL from other adjacent-lying prefrontal cortical subfields. DAPI-treated sections were mounted on nitrocellulose filter paper and submerged in a tissue culture dish containing PBS and viewed under fluorescence using a fixed-stage microscope (Leica DM5500). Injections of 5% Lucifer yellow (Invitrogen) were made by iontophoresis through micropipettes (1–2 μm inner diameter) under a DC current of 1–6 nA for 5–10 min. The placement of injections was evaluated with reference to standard cytoarchitectonic parcellations of PL (Krettek and Price, 1977; Vogt and Peters, 1981). The regions are of primary interest for distinguishing PL from adjacent-lying regions (from dorsal-to-ventral): the dorsal subdivision of the anterior cingulate area (ACd), PL, and IL In DAPI-stained material, the ACd is characterized by a sparse layer 3, and a loosely packed and broad layer 5, which distinguishes it from the more homogeneous layer 5 and large, darkly stained cells that comprise PL. The distinction between PL and IL is enabled by the relatively indistinct lamination pattern that emerges ventrally, and the irregular border between layers 1 and 3 that typify IL.

In all three experiments, neurons in layers 2 and 3 of PL (corresponding to anteroposterior coordinates: 2.9 – 3.5 mm relative to bregma) were selected for the dye injection procedure, whereas experiment 2 involved the selection of neurons in layers 2, 3, and 5. The general technique for cell filling involved carefully observing the passive diffusion of LY resulting from application of a negligibly small amount of current from the advancing micropipette tip under 40× magnification; LY diffuses amorphously until hitting a dendritic process or cell body, whereby the dye becomes restricted intracellularly. After several neurons were filled intracellularly, tissue sections were mounted onto glass slides and coverslipped in Vectashield (Vector Laboratories).

Dendritic morphologic analyses of PL neurons in layers 2 and 3

Neuronal reconstructions were performed for the analysis of quantitative changes in dendritic morphology as a function of the corticosterone treatment regimens employed. Apical dendrites of pyramidal neurons in layers 2 and 3 of PL are morphologically heterogeneous and have been shown to retain relatively consistent quantitative indices (i.e., branch length, number of branch endings) that affords pooling them into a single analysis (Radley et al., 2004; Cook and Wellman, 2004; Liston et al., 2006; Cerqueira et al., 2007). On the other hand, since layer 5 neurons have highly contrasting morphological features (Larkman and Mason, 1990; Kasper et al., 1994; Tsiola et al., 2003; Holtmaat et al., 2006; van Aerde and Feldmeyer, 2015), the dendritic morphologic analyses performed in the

current study were restricted to data sets (i.e., experiments 1 and 3) that encompassed only neurons in layers 2 and 3.

An experimenter unaware of the treatment condition for each animal performed neuronal reconstructions and data analyses. Pyramidal neuron dendritic arbors in layers 2 and 3 of PL were reconstructed in 3D using a computer-assisted morphometry system consisting of a Leica DM4000R equipped with an Applied Scientific Instrumentation MS-2000 XYZ computer-controlled motorized stage, a QImaging Blue digital camera, a Gateway computer, and morphometry software (MBF Biosciences). Neurons were visualized, and the dendritic tree was reconstructed using a Leica Apochromat 40× objective with a numerical aperture (NA) of 1.4 and Neurolucida software (MBF Biosciences; RRID:SCR_001775). To be considered for dendritic morphologic analysis, LY-filled PL neurons had to exhibit complete filling of the arbor, as evidenced by well-defined endings and a minimum amount of truncated branches. Optimal cases involved apical dendritic trajectories that generally coursed parallel to, or gently downward from, the top surface of the section. Truncations in apical dendrites were permitted only in instances where collateral branches were deemed to be nearing the point of termination or un to make any further bifurcations. For basal dendrites, it was common to retain an average of 1–3 entirely intact arbors for a given LY-filled neuron, such that analyses on intact branches were performed for this category. Total length (μm) and number of branch endings for apical and basal dendrites were obtained from each neuronal reconstruction and analyzed as described below.

Confocal laser scanning microscopy and dendritic spine analysis

Two-dimensional renderings for each neuron were obtained using Neurolucida software, as based upon the neuronal reconstruction procedures described above, and a radial distance of 150 μm from the soma was selected as a boundary delineating proximal and distal portions of the dendritic tree. Within these regions, branches were randomly selected for imaging from each neuron for an average of 3 segments per neuron and 5 neurons for each animal. The selection criteria for confocal imaging of dendritic segments are based upon previous reports (Radley et al., 2006; Radley et al., 2013; Anderson et al., 2014): (1) possess a diameter of <3 μm, as larger diameter dendrites in PL pyramidal neurons exhibit greater variability in spine density values; (2) reside within a depth of 70 μm from the top surface of the section, due to the limited working distance of the optical system; (3) to be either parallel to, or course gently relative to, the coronal surface of the section (i.e., this helps to minimize *z*-axis distortion and facilitate the unambiguous identification of spines); and (4) have no overlap with other branches that would obscure visualization of spines. In contrast to the dendritic arborization analyses described above, dye-filled neurons containing truncated branches were permissible for their inclusion into the dendritic spine imaging and analysis, as long as they exhibited complete filling of the dendritic arbor and well-defined branch tips.

z-Stacks were collected on a Leica SP5 confocal laser-scanning microscope equipped with an argon laser and a 100X, 1.4 NA oil-immersion objective, using voxel dimensions of 0.1 × 0.1 × 0.1 μm^3. Settings for pinhole size (1 airy disc), gain, and offset were optimized initially and then held relatively constant throughout the study to ensure that all images were digitized under similar illumination conditions at a resolution of 512 × 512 pixels. Images

were deconvolved with AutoDeblur (Media Cybernetics), and spine analyses were performed using the semiautomated software *NeuronStudio* (Rodriguez et al., 2006; Radley et al., 2008; Rodriguez et al., 2008; Rodriguez et al., 2009; Anderson et al., 2014) (http://research.mssm.edu/cnic/tools-ns.html; RRID:SCR_013798), which analyzes in 3D dendritic length, spine density, and morphometric features (i.e., head/neck diameter, volume, subtype) for each dendritic spine. Spines were classified as thin or mushroom if the ratio of the head diameter-to-neck diameter was >1.1. If their ratio exceeded this value, spines with a maximum head diameter >0.4 μm were classified as mushroom, or else were classified as thin. Spines with head-to-neck diameter ratios <1.1 were also classified as thin if the ratio of spine length-to-neck diameter was >2.5; otherwise, they were classified as stubby. A fourth category, filopodial spines, exhibited a long and thin shape with no enlargement at the distal tip. Since these were very seldom observed, they were classified as thin subtypes. Finally, data readouts from the spine analysis algorithm were visually compared by the experimenter for each optical stack to verify accurate subtype classifications for dendritic spines.

Statistics

Group data from the B radioimmunoassay were compared with a repeated measures ANOVA, followed by pairwise comparisons using Fisher's LSD at both morning and evening time points. Data are expressed as the mean ± SEM. Dendritic branch and spine morphometric data were averaged from each animal (i.e., 3–5 segments/neuron, 5–7 neurons/rat) as a function of treatment. The final group sizes in both experiments were lower than our starting sample sizes reported above. This difference is due to the fact that the success rate from perfused rats that yield suitable numbers of fluorescent dye-filled neurons for inclusion into the analysis is ~55%. The effects on overall dendritic length, number of branch endings, dendritic spine and subtype densities were compared using a one-way ANOVA. Population analysis of spine volume as a function of subtype and experimental treatment were analyzed via comparison of cumulative frequency distributions using the Kolmogorov–Smirnov test with MATLAB software (MathWorks). Additional correlational tests were performed for the assessment of whether each dependent measure varied as a function of integrated B values for each subject, although since no significant trends were identified, these results are not reported here. All pairwise comparisons were made using Fisher's LSD, with significance set at $p < 0.05$, and data are expressed as mean + SEM. Significance for the Kolmogorov-Smirnov test was set at $p < 0.01$.

RESULTS

Experiment 1: Effects of varying doses of corticosterone (B) on structural plasticity in PL

Characterization of plasma B levels—Two weeks after pellet implantation (i.e. 100 mg, 200 mg, or cholesterol) blood samples were collected from the tail vein of rats at times approximating the circadian nadir (0700) and zenith (1700; as determined based upon our pervious characterization of the sex, strain, age, and housing conditions of these rats; Anderson et al., 2014) to verify pellet efficacy and plasma B concentrations relative to intact rats (Fig. 1A). Repeated-measures ANOVA showed main effects for time of day ($F_{(1,19)} = 7.2$, $p < 0.05$) and interaction between time of day and treatment group ($F_{(2,19)} = 10.5$, $p < 0.05$). While B levels held constant throughout the day in ADX + 100B and ADX + 200B

groups, sham ADX rats showed lower AM and increased PM plasma B levels (Fig. 1). Pairwise comparisons revealed plasma levels of B in ADX + 100B and ADX + 200B that were lower in PM and higher in AM, respectively, as compared with sham ADX rats ($p < 0.05$ for each, Fig. 1B). These data suggest resultant plasma B levels in the 100B group that roughly approximated to the circadian mean (9 μg/dl), and the 200B group displaying closer to circadian peak values (14 μg/dl), as compared with sham ADX rats (11 and 16 μg/dl, respectively).

Chronic elevations in plasma B induce dendritic spine loss in PL pyramidal neurons—Figures 2 and 3 illustrate groups of Lucifer yellow-filled pyramidal neurons in layers 2 and 3 of PL that were subjected to dendritic spine morphometric analyses (198, 106, and 109 dendritic segments in sham, 100B, and 200B groups, respectively). These segments yielded a total of 54,267 dendritic spines subjected to density, subtype, and morphologic analysis (sham: N = 10 rats/27,225 spines; 100B: N = 6 rats/14,458 spines; 200B: N = 6 rats/12,554 spines)(Table 1). One-way ANOVA performed at different portions of the dendritic tree revealed most pronounced main effects in distal apical dendrites (i.e., >150 μm; $F_{(2,20)} = 3.873$, $p = 0.04$) (Fig. 4). ADX + 200B rats displayed a 21% decrease in dendritic spine density within this region, and a 13% decrease when combined across all three regions, as compared with sham ADX rats ($p < 0.01$ for each). By contrast, ADX + 100B treatment failed to produce any reliable differences in dendritic spine density relative to control or 200B dose groups (Fig. 4; Table 1).

Further analyses of dendritic arborization patterns (overall length, branch number) in the same set of PL neurons was undertaken to assess the extent to which dendritic spine loss may be accounted for by larger-scale changes in dendritic morphology. This analyses revealed a main effect for apical dendritic length ($F_{(2,20)} = 3.5$, $p = 0.05$). *Post-hoc* comparisons revealed a 23% reduction in apical dendritic length in B200 rats relative to sham control rats ($p = 0.02$), whereas no significant reduction was evident between B100 and sham control groups ($p = 0.2$)(Fig. 5). Prolonged B exposure failed to alter the number of branch endings in apical dendrites, and also had no effect on either index in basal dendrites (Fig. 5; Table 1). When apical dendritic shortening and decreases in spine density are taken together, this compounds the net loss of dendritic spines in layers 2 and 3 PL neurons to levels approximating 67% to control values following prolonged high-dose exposure of glucocorticoids.

Effects of high levels of B on PL dendritic spine morphology—Dendritic spines can be distinguished by geometric characteristics (i.e., thin, mushroom, stubby) that have proven to be useful for inferring synaptic structure-function relationships (Kasai et al., 2003; Bourne and Harris, 2007; Yang et al., 2009; Dumitriu et al., 2010; Lee et al., 2012; Fig. 5A). In cortical pyramidal neurons, spines classified as thin represent the majority of the population (60–70%; Bourne and Harris, 2007), and previous studies have identified this subtype as important for LTP and learning-related plasticity (Arnsten et al., 2010; Anderson et al., 2014). In our analysis of spine subtype (Fig. 6A), thin spines were the most vulnerable to prolonged high-dose glucocorticoid exposure, particularly within more distal apical dendrites ($F_{(2,20)} = 3.6$, $p < 0.05$). *Post-hoc* comparisons revealed a significant 15%

decrement of thin spines in combined apical and basal segments in the 200B group as compared with control rats ($p < 0.05$), with the most significant loss on the most distal aspects (by 24%, $p < 0.05$)(Fig. 6B). By contrast, examination of thin spine densities in the 100B group failed to demonstrate any reliable shifts relative to control or 200B rats (Fig. 6B; Table 1).

Evaluation of other spine subtypes (mushroom, stubby) did not uncover any differences following prolonged glucocorticoid exposure (Fig. 6C, D). Moreover, additional analyses of several spine parameters (length, head diameter, volume) did not reveal any group differences as a function of glucocorticoid treatment (data not shown). However, population analysis of spine volume revealed cumulative frequency shifts following both regimens of glucocorticoid treatment. Comparison of frequency distributions of overall spine populations revealed downward trends (i.e., leftward shifts) in volume in both 100B and 200B relative to control groups (Kolmogorov-Smirnov test, K–S; $p = 0.02$ and $p < 0.01$, respectively), with the 200B spine population showing an even further shift relative to 100B (K–S test, $p < 0.01$)(Fig. 7A). Examination of frequency shifts in subtypes revealed the greatest effects in thin spines (Fig. 7B); 100B showed a leftward shift relative to controls (K–S test, $p < 0.01$), whereas 200B showed significant shifts relative to both control and 100B populations (K–S test, $p < 0.01$ for each). Cumulative frequencies plotted for mushroom spine subtypes also revealed a leftward shift in the 200B treatment group relative to 100B and control groups (K–S test, $p < 0.01$ for each), whereas the 100B group failed to show any differences in this index relative to the control population (K–S test, $p = 0.7$)(Fig. 7C). These observations support the interpretation that prolonged B exposure induces dendritic spine shrinkage in PL neurons, even in the absence of any frank loss of spines in the case of low-dose B, whereas high-dose B results in more generalized decreases in spine volume across subtypes as well as attrition of thin spines.

Experiment 2: Persistence of B-induced structural alterations in PL following a 3-week recovery period

Characterization of plasma B levels—Next, we examined whether a washout period following prolonged B exposure would ameliorate the regressive structural alterations in PL dendritic spines (Fig. 8A). In this experiment, we extended our spine morphologic analysis to include neurons in layers 2, 3, and 5, to assess the extent to which glucocorticoid-induced spine loss generalizes across different laminae in PL. On day 14 after steroid implantation, blood samples were collected from the tail vein of rats in the control and 200B + recovery groups to verify pellet efficacy and plasma B concentrations, and blood samples were collected again on day 35 (i.e., in 200B and 200B + recovery groups) to verify the normalization of adrenocortical activity during the washout period. Repeated-measures ANOVA showed main effects for treatment group ($F_{(3,45)} = 5.3$, $p < 0.05$), time of day ($F_{(1,45)} = 7.2$, $p < 0.05$), and interaction ($F_{(3,45)} = 24.0$, $p < 0.05$). B levels remained consistently elevated near the circadian zenith during the 21 day B exposure time frame in both 200B and 200B + recovery groups, as compared with sham controls (Fig. 8B). 200B + recovery rats displayed normalization of AM and PM levels of plasma B when assayed during the washout period on day 35 (Fig. 8B).

Lack of normalization in PL dendritic spine morphology following recovery from B exposure—In this experiment, 460 dendritic segments from 153 fluorescent dye-labeled PL neurons in layers 2, 3, and 5 were analyzed for spine density and morphometric analysis (120, 160, and 180 dendritic segments in control, 200B, and 200B + recovery groups, respectively). These segments yielded a total of 61,600 dendritic spines subjected to density, subtype, and morphologic analysis (sham: N = 6 rats/17,400 spines; 200B: N = 7 rats/20,800 spines; 200B + recovery: N = 8 rats/23,400 spines)(Table 2). One-way ANOVA of spine density in layers 2, 3, and 5 pyramidal neurons revealed a main effect as a function of experimental treatment ($F_{(2,18)} = 4.6$, $p < 0.05$)(Fig. 9, A–C). *Post-hoc* analyses revealed significant decreases in 200B and 200B + recovery groups relative to controls (by 16%, $p < 0.05$ for each)(Fig. 9C), suggesting that a 21-day washout period was insufficient to reverse glucocorticoid-induced decrements in spine density even after normalization of circadian adrenocortical activity. Regional analysis of apical and basal subdivisions demonstrated downward trends throughout, with statistically significant reductions evident in the proximal region of the apical tree in the 200B group ($p < 0.05$), and basal dendrites of 200B + recovery group ($p < 0.05$), relative to controls. By contrast, no trends or statistically significant differences in spine density were evident in 200B and 200B + recovery groups.

Examination of spine subtype revealed generalized downward trends in both 200B and 200B + recovery groups. These effects were most noteworthy in overall mushroom ($F_{(2,18)} = 3.5$, $p = 0.052$) and overall thin ($F_{(2,18)} = 2.8$, $p = 0.08$) categories, however, neither were statistically significant (Fig. 9, D–F). Follow-up analysis of population shifts in spine volume revealed a significant decrements in both 200B and 200B + recovery groups when compared to control animals (K–S test, $p < 0.01$ for each), whereas the frequency distributions between 200B and 200B + recovery were not statistically different (K–S test, $p = 0.11$)(Fig. 10A). Population analyses performed within thin and mushroom spines also revealed similar leftward (downward) shifts in volume in 200B and 200B + recovery groups relative to controls (K–S test, $p < 0.01$ for each), whereas no statistically significant differences were noted via comparison of cumulative distributions between 200B and 200B + recovery (Fig. 10B, C). These data endorse the results from the first experiment that high-dose glucocorticoid exposure may induce a persistent attrition of dendritic spines throughout pyramidal neurons in PL, likely via one or multiple mechanisms involving spine pruning and shrinkage.

Experiment 3: Effects of short-term B exposure on structural plasticity in PL

As the first two experiments demonstrate that 2 weeks or longer of prolonged high-dose glucocorticoid exposure induces regressive structural plasticity in PL neurons, in a final experiment we addressed whether a shorter duration (i.e., 1 week) of high-dose B exposure could produce similar changes. In these studies, we again restricted our analyses to PL neurons within layers 2 and 3 in order to compare both dendritic morphology and spine density. Nevertheless, this analysis failed to reveal any effects on any of the structural indices examined (Fig. 11; Table 3). These data, when taken together with the other two experiments, suggest that >1 week of continuous exposure to glucocorticoids is necessary for the induction of regressive modifications in PL neurons.

DISCUSSION

It has been widely documented that chronic stress leads to the reorganization of neuronal architecture in mPFC. Here we expand on these findings by showing that increasing plasma levels of B over a period of at least 2 weeks induces apical dendritic shortening, spine loss, and morphological alterations in PL pyramidal neurons. A more surprising result is that these structural alterations persist, even after a washout period and its attendant restoration of circadian B secretory activity. These data generally endorse the view that chronic stress-induced effects on prefrontal structural plasticity involve a glucocorticoid-dependent component. However, they contrast with the effects of repeated stress, whereby recovery periods restored dendrite and spine morphologic indices (Radley et al., 2005; Bloss et al., 2010; Bloss et al., 2011). It is worth emphasizing that prolonged elevations in glucocorticoids are not taken to be equivalent to stress. In fact, elevated glucocorticoids may be more broadly representative of dysregulated homeostatic parameters produced by systemic diseases or by prolonged pharmacotherapeutic regimens in certain chronic conditions. Therefore, our data implicate disrupted adrenocortical function in the induction of protracted synaptic reorganization in mPFC that may follow prolonged stress or other diseases involving endocrine disruptions.

Methodological considerations

A variety of repeated stress manipulations are known to reliably decrease dendrite and spine morphologic indices throughout mPFC subfields in the rat (Cook and Wellman, 2004; Radley et al., 2004; Liston et al., 2006; Michelsen et al., 2007; Perez-Cruz et al., 2007; Liu and Aghajanian, 2008; Radley et al., 2008; Dias-Ferreira et al., 2009; Hains et al., 2009; Holmes and Wellman, 2009; Shansky et al., 2009). However, previous work investigating the effects of repeated B exposure on mPFC structural plasticity has produced mixed results. In one series of studies, repeated daily glucocorticoid injections for 3 weeks differentially altered mPFC pyramidal neuron dendritic morphology, marked by increased and decreased dendritic branching patterns in proximal and distal aspects of the dendritic tree, respectively, and increased dendritic spine density in the same cell types (Wellman, 2001; Seib and Wellman, 2003). Another report found decreased dendrite length, branching patterns, and anatomical regional volumes in mPFC subfields, with no change in spine density following one month of daily glucocorticoid injections (Cerqueira et al., 2005; Cerqueira et al., 2007). By contrast, studies that have administered corticosteroids through the drinking water for 10–20 days have also observed mPFC spine density decrements comparable to those induced by stress (Liu and Aghajanian, 2008; Gourley et al., 2013). While it is possible that some of these discrepancies are attributable to varying modes of glucocorticoid administration (i.e., injections, drinking water, subcutaneous implants), different approaches for visualization and quantification spines are also likely contributors. For instance, much of the information from this field of study is derived from the Golgi impregnation method, yet recent evidence suggests that this approach undersamples dendritic spine densities (by >50%) and specifically biases against the identification of thin subtypes (for a discussion of this issue, see Dumitriu et al., 2011; Dumitriu et al., 2012; Radley et al., 2015). Nevertheless, the present results and the weight of prior evidence support our interpretation

that prolonged glucocorticoid exposure leads to regressive and persistent dendritic spine alterations in mPFC neurons.

Our study also highlights the importance of applying more refined technical approaches to better understand glucocorticoid effects on structural plasticity. In another line of investigation, Liston and Gan (2011) applied two-photon microscopy for time-lapse imaging of dendritic spines in the mouse somatosensory cortex (S1) to show that prolonged glucocorticoid exposure concurrently eliminated existing spines and prevented new spine formation. Although there are some constraints in the level of resolution that is currently achievable with *in vivo* two-photon microscopy, the ability to perform repeated sampling has provided fundamentally important information regarding how glucocorticoids influence spine dynamics (Liston et al., 2013). Electron microscopic approaches will continue to provide important ultrastructural detail for understanding glucocorticoid effects on synaptic alterations, and emerging developments in automated technologies may soon enable higher throughput screening at this level of resolution (e.g., see Kasthuri et al., 2015). In the meantime, the dendritic spine morphometric approach employed here balances the attainment of high quality resolution with high-throughput that cannot yet be achieved with other methods.

Interpretive considerations

Comparing and contrasting data from each of the experiments presented in this report raises some interesting questions regarding possible differences in effects of glucocorticoids on dendritic spine alterations. First, we failed to observe consistent decreases in thin spine subtypes as a function of glucocorticoids across both experiments. In the initial experiment, high-dose treatment of B for 2 weeks induced significant decrements in spine density that were manifested by a clear loss of thin spines in PL neurons, whereas in the second experiment, 3-week B exposure failed to result in a statistically significant reduction in this subtype (e.g., Fig. 9D). This is likely due to the fact that the former experiment examined of only layer 3 PL neurons, and the latter involved the analysis of both layer 3 and 5 PL neurons. Since we often observe lower overall spine densities in layer 5 relative to 3 pyramidal neurons in mPFC (Anderson and Radley, unpublished observations), combining these into one analysis may have increased the variance enough to reduce the reliability of the observed effects. Given that experience-dependent dendritic spine plasticity has been shown to vary as a function of apical dendritic morphology in layer 5 neurons in S1 (Holtmaat et al., 2006), it is possible that our failure to examine dendritic morphology in layer 5 PL neurons, or partition subpopulations accordingly, added an additional source of variability in experiment two.

A second interpretive issue concerns whether rats that were subjected to a longer period of B exposure (i.e., 3 weeks in the second experiment as opposed to 2 weeks in the first), may have shown greater spine loss in PL. While there were no frank differences in the overall proportion of spines lost between experiments (by 13% and 16% in experiments one and two, respectively), the second experiment revealed more expansive downward trends in both thin ($p = 0.08$) and mushroom ($p = 0.052$) subtypes, whereas the first displayed only decreases in thin, and no downward trend in mushroom subtypes. Since mushroom spines

are representative of a category of larger volume, stable, and mature synaptic phenotypes (Harris and Stevens, 1989; Kasai et al., 2003; Holtmaat et al., 2005; Knott et al., 2006; Yasumatsu et al., 2008), one possibility is that B-induced spine shrinkage of this subtype requires longer intervals of steroid exposure. In this scenario, mushroom spine shrinkage could fall below our threshold criteria for being classified as mushroom (i.e., spine head diameter > 0.4 μm; see Methods for further details), resulting in their reclassification as "thin." The idea that an extended period of glucocorticoid exposure can lead to the selective targeting of large volume spines is supported by at least two studies (Tanokashira et al., 2012; Liston et al., 2013), and may involve rearrangement of the F-actin network in the spine head via downregulation of the stabilizing protein caldesmon (Tanokashira et al., 2012). This caldesmon-dependent signaling pathway underlying spine shrinkage is also distinct from the aforementioned mechanisms for spine formation/elimination, which raises the possibility that the spine loss and shrinkage we observed following high-dose B treatment may be regulated via distinct mechanisms. Support for this idea might also derive from the observation that prolonged lower-dose B treatment in the first experiment resulted in reliable decreases only in spine volume.

Our results in the second experiment show that 3 weeks of repeated B exposure dendritic spine alterations were evident even in rats provided with a 3-week washout period that allowed for the normalization of HPA rhythmicity after high-dose B exposure. At least one previous report has shown that dendritic spine decreases in prefrontal subfields exhibit regionally differentiated patterns of partial recovery following prolonged B exposure (i.e., in infralimbic but not orbitofrontal cortex) after a 7-day washout period (Gourley et al., 2013). One possibility is that PL may be less resilient to corticosteroid-induced dendritic spine alterations even the restoration of HPA rhythmicity, although more work is needed to better understand how stressful or traumatic experiences may induce long-lasting disruptions in prefrontal networks.

The data presented here may also help to conceptualize how hypercortisolism in Cushing's syndrome or aging could lead to enduring regressive structural and functional changes in mPFC synaptic networks. Patients of Cushing's syndrome display cognitive and prefrontal functional deficits that linger after the normalization of glucocorticoids (for review see Andela et al., 2015) (Tiemensma et al., 2010a; Tiemensma et al., 2010b). Recent evidence suggests that diminished prefrontal functional connectivity and cortical thinning in Cushing's syndrome persist even after long-term remission of elevated glucocorticoids (Crespo et al., 2014; Bas-Hoogendam et al., 2015). The cumulative exposure to glucocorticoids in rats has also recently been implicated in age-related decreases in dendritic spine density in mPFC and prefrontal functioning (Anderson et al., 2014), whereas many studies have linked elevated glucocorticoids in aging with hippocampal and prefrontal impairments (e.g., see Landfield, 1978; Issa et al., 1990; Sapolsky, 1992; Lupien et al., 1994; Mizoguchi et al., 2009; Franz et al., 2011; Garrido et al., 2012).

Role of disruptions in the adrenocortical rhythm

One lingering question concerns the extent to which B-mediated prefrontal structural alterations may be explained by elevated plasma levels *per se*, or the resultant disruption of

circadian rhythmicity due to the continuous release of steroid into the circulation achieved with subcutaneous implants. As HPA axis dysregulation may often reflect a flattening of the B secretory rhythm in a variety of human clinical disorders (e.g., see Miller et al., 2007; Hall et al., 2015), this may have relevance to the repeated glucocorticoid regimen used in the present study. Studies utilizing other methods of repeated B administration that likely enhance circadian peaks of B have also observed similar effects on structural plasticity (Liu and Aghajanian, 2008; Liston and Gan, 2011; Gourley et al., 2013; Swanson et al., 2013), although information is not yet forthcoming regarding the precise morphological differences in spine volume and subtype under these varying regimens of glucocorticoid treatment. Several recent studies have linked glucocorticoid circadian rhythmicity to natural variations in spine formation and elimination (i.e., in somatosensory cortex and hippocampus)(Liston et al., 2013; Ikeda et al., 2015). In two other reports, disruption of the circadian photoperiod induced regressive structural changes in hippocampal and mPFC, along with corresponding cognitive impairments (Pyter et al., 2005; Karatsoreos et al., 2011). These latter studies warrant consideration of whether changes in adrenocortical secretory patterns underlie cognitive impairments following circadian disruption, and the extent to which changes in circadian secretory patterns, versus increased levels of B, account for prefrontal structural and functional alterations in other experimental and clinical contexts.

Functional considerations

Thin spine subtypes in prefrontal neurons have proven to be highly vulnerable to pruning in response to a variety of contexts, including aging and chronic stress (Dumitriu et al., 2010; Bloss et al., 2011; Radley et al., 2013; Anderson et al., 2014). More recently, thin spine loss in the prefrontal cortex has been implicated in psychiatric illnesses such as schizophrenia as well as psychostimulant use (Arnsten et al., 2010; McEwen and Morrison, 2013; Radley et al., 2015), and our data implicate altered adrenocortical functioning as a contributing factor to prefrontal synaptic reorganization in these settings. One important question concerns whether prolonged glucocorticoid exposure decreases thin spines through a mechanism involving impaired spine formation and/or increased elimination. Recent evidence suggests that short-term exposure to glucocorticoids mediates both processes via separate signaling pathways; spine formation via glucocorticoid receptor (GR) type I activation via a LIM kinase-cofillin pathway, and spine elimination through a GR type II transcriptionally dependent mechanism (Liston et al., 2013). Future studies are needed to better understand the precise mechanisms underlying prefrontal spine attrition in response to prolonged periods of glucocorticoid exposure, chronic stress, and other contexts involving altered adrenocortical functioning.

Acknowledgments

This work was supported by National Institutes of Health MH-095972 (J.J.R.), and NARSAD Independent Investigator Grants (J.J.R.).

References

Alfarez DN, De Simoni A, Velzing EH, Bracey E, Joels M, Edwards FA, Krugers HJ. Corticosterone reduces dendritic complexity in developing hippocampal CA1 neurons. Hippocampus. 2009; 19(9): 828–836. [PubMed: 19235231]

Andela CD, van Haalen FM, Ragnarsson O, Papakokkinou E, Johannsson G, Santos A, Webb SM, Biermasz NR, van der Wee NJ, Pereira AM. MECHANISMS IN ENDOCRINOLOGY: Cushing's syndrome causes irreversible effects on the human brain: a systematic review of structural and functional magnetic resonance imaging studies. Eur J Endocrinol. 2015; 173(1):R1–14. [PubMed: 25650405]

Anderson RM, Birnie AK, Koblesky NK, Romig-Martin SA, Radley JJ. Adrenocortical status predicts the degree of age-related deficits in prefrontal structural plasticity and working memory. The Journal of neuroscience: the official journal of the Society for Neuroscience. 2014; 34(25):8387–8397. [PubMed: 24948795]

Antoni FA. Hypothalamic control of adrenocorticotropin secretion: advances since the discovery of 41-residue corticotropin-releasing factor. Endocr Rev. 1986; 7(4):351–378. [PubMed: 3023041]

Arnsten AF, Paspalas CD, Gamo NJ, Yang Y, Wang M. Dynamic Network Connectivity: A new form of neuroplasticity. Trends in cognitive sciences. 2010; 14(8):365–375. [PubMed: 20554470]

Bas-Hoogendam JM, Andela CD, van der Werff SJ, Pannekoek JN, van Steenbergen H, Meijer OC, van Buchem MA, Rombouts SA, van der Mast RC, Biermasz NR, van der Wee NJ, Pereira AM. Altered neural processing of emotional faces in remitted Cushing's disease. Psychoneuroendocrinology. 2015; 59:134–146. [PubMed: 26092780]

Bloss EB, Janssen WG, McEwen BS, Morrison JH. Interactive effects of stress and aging on structural plasticity in the prefrontal cortex. The Journal of neuroscience: the official journal of the Society for Neuroscience. 2010; 30(19):6726–6731. [PubMed: 20463234]

Bloss EB, Janssen WG, Ohm DT, Yuk FJ, Wadsworth S, Saardi KM, McEwen BS, Morrison JH. Evidence for reduced experience-dependent dendritic spine plasticity in the aging prefrontal cortex. The Journal of neuroscience: the official journal of the Society for Neuroscience. 2011; 31(21): 7831–7839. [PubMed: 21613496]

Bourne J, Harris KM. Do thin spines learn to be mushroom spines that remember? Current opinion in neurobiology. 2007; 17(3):381–386. [PubMed: 17498943]

Cerqueira JJ, Pego JM, Taipa R, Bessa JM, Almeida OF, Sousa N. Morphological correlates of corticosteroid-induced changes in prefrontal cortex-dependent behaviors. The Journal of neuroscience: the official journal of the Society for Neuroscience. 2005; 25(34):7792–7800. [PubMed: 16120780]

Cerqueira JJ, Taipa R, Uylings HB, Almeida OF, Sousa N. Specific configuration of dendritic degeneration in pyramidal neurons of the medial prefrontal cortex induced by differing corticosteroid regimens. Cerebral cortex. 2007; 17(9):1998–2006. [PubMed: 17082516]

Cook SC, Wellman CL. Chronic stress alters dendritic morphology in rat medial prefrontal cortex. Journal of neurobiology. 2004; 60(2):236–248. [PubMed: 15266654]

Crespo I, Esther GM, Santos A, Valassi E, Yolanda VG, De Juan-Delago M, Webb SM, Gomez-Anson B, Resmini E. Impaired decision-making and selective cortical frontal thinning in Cushing's syndrome. Clin Endocrinol (Oxf). 2014; 81(6):826–833. [PubMed: 25052342]

Dias-Ferreira E, Sousa JC, Melo I, Morgado P, Mesquita AR, Cerqueira JJ, Costa RM, Sousa N. Chronic stress causes frontostriatal reorganization and affects decision-making. Science. 2009; 325(5940):621–625. [PubMed: 19644122]

Diorio D, Viau V, Meaney MJ. The role of the medial prefrontal cortex (cingulate gyrus) in the regulation of hypothalamic-pituitary-adrenal responses to stress. The Journal of neuroscience: the official journal of the Society for Neuroscience. 1993; 13(9):3839–3847. [PubMed: 8396170]

Dumitriu D, Hao J, Hara Y, Kaufmann J, Janssen WG, Lou W, Rapp PR, Morrison JH. Selective changes in thin spine density and morphology in monkey prefrontal cortex correlate with aging-related cognitive impairment. The Journal of neuroscience: the official journal of the Society for Neuroscience. 2010; 30(22):7507–7515. [PubMed: 20519525]

Dumitriu D, Laplant Q, Grossman YS, Dias C, Janssen WG, Russo SJ, Morrison JH, Nestler EJ. Subregional, dendritic compartment, and spine subtype specificity in cocaine regulation of dendritic spines in the nucleus accumbens. The Journal of neuroscience: the official journal of the Society for Neuroscience. 2012; 32(20):6957–6966. [PubMed: 22593064]

Dumitriu D, Rodriguez A, Morrison JH. High-throughput, detailed, cell-specific neuroanatomy of dendritic spines using microinjection and confocal microscopy. Nat Protoc. 2011; 6(9):1391–1411. [PubMed: 21886104]

Feldman S, Conforti N. Participation of the dorsal hippocampus in the glucocorticoid feedback effect on adrenocortical activity. Neuroendocrinology. 1980; 30(1):52–55. [PubMed: 7354890]

Franz CE, O'Brien RC, Hauger RL, Mendoza SP, Panizzon MS, Prom-Wormley E, Eaves LJ, Jacobson K, Lyons MJ, Lupien S, Hellhammer D, Xian H, Kremen WS. Cross-sectional and 35-year longitudinal assessment of salivary cortisol and cognitive functioning: the Vietnam Era twin study of aging. Psychoneuroendocrinology. 2011; 36(7):1040–1052. [PubMed: 21295410]

Gabbott PL, Warner TA, Jays PR, Salway P, Busby SJ. Prefrontal cortex in the rat: projections to subcortical autonomic, motor, and limbic centers. The Journal of comparative neurology. 2005; 492(2):145–177. [PubMed: 16196030]

Garrido P, De Blas M, Gine E, Santos A, Mora F. Aging impairs the control of prefrontal cortex on the release of corticosterone in response to stress and on memory consolidation. Neurobiology of aging. 2012; 33(4):827 e821–829.

Gourley SL, Swanson AM, Koleske AJ. Corticosteroid-induced neural remodeling predicts behavioral vulnerability and resilience. The Journal of neuroscience: the official journal of the Society for Neuroscience. 2013; 33(7):3107–3112. [PubMed: 23407965]

Grillo CA, Risher M, Macht VA, Bumgardner AL, Hang A, Gabriel C, Mocaer E, Piroli GG, Fadel JR, Reagan LP. Repeated restraint stress-induced atrophy of glutamatergic pyramidal neurons and decreases in glutamatergic efflux in the rat amygdala are prevented by the antidepressant agomelatine. Neuroscience. 2015; 284:430–443. [PubMed: 25280788]

Hains AB, Vu MA, Maciejewski PK, van Dyck CH, Gottron M, Arnsten AF. Inhibition of protein kinase C signaling protects prefrontal cortex dendritic spines and cognition from the effects of chronic stress. Proceedings of the National Academy of Sciences of the United States of America. 2009; 106(42):17957–17962. [PubMed: 19805148]

Hall BS, Moda RN, Liston C. Glucocorticoid Mechanisms of Functional Connectivity Changes in Stress-Related Neuropsychiatric Disorders. Neurobiology of stress. 2015; 1:174–183. [PubMed: 25729760]

Harris KM, Stevens JK. Dendritic spines of CA 1 pyramidal cells in the rat hippocampus: serial electron microscopy with reference to their biophysical characteristics. The Journal of neuroscience: the official journal of the Society for Neuroscience. 1989; 9(8):2982–2997. [PubMed: 2769375]

Herman JP, Cullinan WE, Morano MI, Akil H, Watson SJ. Contribution of the ventral subiculum to inhibitory regulation of the hypothalamo-pituitary-adrenocortical axis. Journal of neuroendocrinology. 1995; 7(6):475–482. [PubMed: 7550295]

Hinwood M, Morandini J, Day TA, Walker FR. Evidence that microglia mediate the neurobiological effects of chronic psychological stress on the medial prefrontal cortex. Cerebral cortex. 2012; 22(6):1442–1454. [PubMed: 21878486]

Holmes A, Wellman CL. Stress-induced prefrontal reorganization and executive dysfunction in rodents. Neuroscience and biobehavioral reviews. 2009; 33(6):773–783. [PubMed: 19111570]

Holtmaat AJ, Trachtenberg JT, Wilbrecht L, Shepherd GM, Zhang X, Knott GW, Svoboda K. Transient and persistent dendritic spines in the neocortex in vivo. Neuron. 2005; 45(2):279–291. [PubMed: 15664179]

Ikeda M, Hojo Y, Komatsuzaki Y, Okamoto M, Kato A, Takeda T, Kawato S. Hippocampal spine changes across the sleep-wake cycle: corticosterone and kinases. The Journal of endocrinology. 2015; 226(2):M13–27. [PubMed: 26034071]

Issa AM, Rowe W, Gauthier S, Meany MJ. Hypothalamic-pituitary-adrenal activity in aged, cognitively impaired and cognitively unimpaired rats. The Journal of neuroscience: the official journal of the Society for Neuroscience. 1990; 10(10):3247–3254. [PubMed: 2170594]

Jaferi A, Bhatnagar S. Corticosterone can act at the posterior paraventricular thalamus to inhibit hypothalamic-pituitary-adrenal activity in animals that habituate to repeated stress. Endocrinology. 2006; 147(10):4917–4930. [PubMed: 16809449]

Karatsoreos IN, Bhagat S, Bloss EB, Morrison JH, McEwen BS. Disruption of circadian clocks has ramifications for metabolism, brain, and behavior. Proceedings of the National Academy of Sciences of the United States of America. 2011; 108(4):1657–1662. [PubMed: 21220317]

Kasai H, Matsuzaki M, Noguchi J, Yasumatsu N, Nakahara H. Structure–stability–function relationships of dendritic spines. Trends in neurosciences. 2003; 26(7):360–368. [PubMed: 12850432]

Kasthuri N, Hayworth KJ, Berger DR, Schalek RL, Conchello JA, Knowles-Barley S, Lee D, Vazquez-Reina A, Kaynig V, Jones TR, Roberts M, Morgan JL, Tapia JC, Seung HS, Roncal WG, Vogelstein JT, Burns R, Sussman DL, Priebe CE, Pfister H, Lichtman JW. Saturated Reconstruction of a Volume of Neocortex. Cell. 2015; 162(3):648–661. [PubMed: 26232230]

Knott GW, Holtmaat A, Wilbrecht L, Welker E, Svoboda K. Spine growth precedes synapse formation in the adult neocortex in vivo. Nature neuroscience. 2006; 9(9):1117–1124. [PubMed: 16892056]

Krettek JE, Price JL. Projections from the Amygdaloid Complex to the Cerebral Cortex and Thalamus in the Rat and Cat. The Journal of comparative neurology. 1977; 172:687–722. [PubMed: 838895]

Landfield PW. An endocrine hypothesis of brain aging and studies on brain-endocrine correlations and monosynaptic neurophysiology during aging. Adv Exp Med Biol. 1978; 113:179–199. [PubMed: 753087]

Lee KF, Soares C, Beique JC. Examining form and function of dendritic spines. Neural Plast. 2012; 2012:704103. [PubMed: 22577585]

Liston C, Cichon JM, Jeanneteau F, Jia Z, Chao MV, Gan WB. Circadian glucocorticoid oscillations promote learning-dependent synapse formation and maintenance. Nature neuroscience. 2013; 16(6):698–705. [PubMed: 23624512]

Liston C, Gan WB. Glucocorticoids are critical regulators of dendritic spine development and plasticity in vivo. Proceedings of the National Academy of Sciences of the United States of America. 2011; 108(38):16074–16079. [PubMed: 21911374]

Liston C, Miller MM, Goldwater DS, Radley JJ, Rocher AB, Hof PR, Morrison JH, McEwen BS. Stress-induced alterations in prefrontal cortical dendritic morphology predict selective impairments in perceptual attentional set-shifting. The Journal of neuroscience: the official journal of the Society for Neuroscience. 2006; 26(30):7870–7874. [PubMed: 16870732]

Liu RJ, Aghajanian GK. Stress blunts serotonin- and hypocretin-evoked EPSCs in prefrontal cortex: role of corticosterone-mediated apical dendritic atrophy. Proceedings of the National Academy of Sciences of the United States of America. 2008; 105(1):359–364. [PubMed: 18172209]

Lupien SJ, Lecours AR, Lussier I, Schwartz G, Nair NPV, Meany MJ. Basal cortisol levels and cognitive deficits in human aging. The Journal of neuroscience: the official journal of the Society for Neuroscience. 1994; 14(5):2893–2903. [PubMed: 8182446]

McEwen BS. Protective and damaging effects of stress mediators. N Engl J Med. 1998; 338(3):171–179. [PubMed: 9428819]

McEwen BS, Morrison JH. The brain on stress: vulnerability and plasticity of the prefrontal cortex over the life course. Neuron. 2013; 79(1):16–29. [PubMed: 23849196]

McIntyre CK, Power AE, Roozendaal B, McGaugh JL. Role of the basolateral amygdala in memory consolidation. Ann N Y Acad Sci. 2003; 985:273–293. [PubMed: 12724165]

McKlveen JM, Myers B, Flak JN, Bundzikova J, Solomon MB, Seroogy KB, Herman JP. Role of prefrontal cortex glucocorticoid receptors in stress and emotion. Biological psychiatry. 2013; 74(9):672–679. [PubMed: 23683655]

Michelsen KA, van den Hove DL, Schmitz C, Segers O, Prickaerts J, Steinbusch HW. Prenatal stress and subsequent exposure to chronic mild stress influence dendritic spine density and morphology in the rat medial prefrontal cortex. BMC Neurosci. 2007; 8:107. [PubMed: 18093285]

Miller GE, Chen E, Zhou ES. If it goes up, must it come down? Chronic stress and the hypothalamic-pituitary-adrenocortical axis in humans. Psychological bulletin. 2007; 133(1):25–45. [PubMed: 17201569]

Mitra R, Jadhav S, McEwen BS, Vyas A, Chattarji S. Stress duration modulates the spatiotemporal patterns of spine formation in the basolateral amygdala. Proceedings of the National Academy of Sciences of the United States of America. 2005; 102(26):9371–9376. [PubMed: 15967994]

Mitra R, Sapolsky RM. Acute corticosterone treatment is sufficient to induce anxiety and amygdaloid dendritic hypertrophy. Proceedings of the National Academy of Sciences of the United States of America. 2008; 105(14):5573–5578. [PubMed: 18391224]

Mizoguchi K, Ikeda R, Shoji H, Tanaka Y, Maruyama W, Tabira T. Aging attenuates glucocorticoid negative feedback in rat brain. Neuroscience. 2009; 159(1):259–270. [PubMed: 19141312]

Mizoguchi K, Yuzurihara M, Ishige A, Sasaki H, Chui D, Tabira T. Chronic stress induces impairment of spatial working memory because of prefrontal dopaminergic dysfunction. The Journal of neuroscience: the official journal of the Society for Neuroscience. 2000; 20(4):1568–1574. [PubMed: 10662846]

Morales-Medina JC, Sanchez F, Flores G, Dumont Y, Quirion R. Morphological reorganization after repeated corticosterone administration in the hippocampus, nucleus accumbens and amygdala in the rat. J Chem Neuroanat. 2009; 38(4):266–272. [PubMed: 19505571]

Perez-Cruz C, Muller-Keuker JI, Heilbronner U, Fuchs E, Flugge G. Morphology of pyramidal neurons in the rat prefrontal cortex: lateralized dendritic remodeling by chronic stress. Neural Plast. 2007; 2007:46276. [PubMed: 18253468]

Pyter LM, Reader BF, Nelson RJ. Short photoperiods impair spatial learning and alter hippocampal dendritic morphology in adult male white-footed mice (Peromyscus leucopus). The Journal of neuroscience: the official journal of the Society for Neuroscience. 2005; 25(18):4521–4526. [PubMed: 15872099]

Radley JJ, Anderson RM, Cosme CV, Glanz RM, Miller MC, Romig-Martin SA, LaLumiere RT. The Contingency of Cocaine Administration Accounts for Structural and Functional Medial Prefrontal Deficits and Increased Adrenocortical Activation. The Journal of neuroscience: the official journal of the Society for Neuroscience. 2015; 35(34):11897–11910. [PubMed: 26311772]

Radley JJ, Anderson RM, Hamilton BA, Alcock JA, Romig-Martin SA. Chronic stress-induced alterations of dendritic spine subtypes predict functional decrements in an hypothalamo-pituitary-adrenal-inhibitory prefrontal circuit. The Journal of neuroscience: the official journal of the Society for Neuroscience. 2013; 33(36):14379–14391. [PubMed: 24005291]

Radley JJ, Rocher AB, Janssen WG, Hof PR, McEwen BS, Morrison JH. Reversibility of apical dendritic retraction in the rat medial prefrontal cortex following repeated stress. Exp Neurol. 2005; 196(1):199–203. [PubMed: 16095592]

Radley JJ, Rocher AB, Miller M, Janssen WG, Liston C, Hof PR, McEwen BS, Morrison JH. Repeated stress induces dendritic spine loss in the rat medial prefrontal cortex. Cerebral cortex. 2006; 16(3):313–320. [PubMed: 15901656]

Radley JJ, Rocher AB, Rodriguez A, Ehlenberger DB, Dammann M, McEwen BS, Morrison JH, Wearne SL, Hof PR. Repeated stress alters dendritic spine morphology in the rat medial prefrontal cortex. The Journal of comparative neurology. 2008; 507(1):1141–1150. [PubMed: 18157834]

Radley JJ, Sisti HM, Hao J, Rocher AB, McCall T, Hof PR, McEwen BS, Morrison JH. Chronic behavioral stress induces apical dendritic reorganization in pyramidal neurons of the medial prefrontal cortex. Neuroscience. 2004; 125(1):1–6. [PubMed: 15051139]

Rodriguez A, Ehlenberger DB, Dickstein DL, Hof PR, Wearne SL. Automated three-dimensional detection and shape classification of dendritic spines from fluorescence microscopy images. PLoS One. 2008; 3(4):e1997. [PubMed: 18431482]

Rodriguez A, Ehlenberger DB, Hof PR, Wearne SL. Rayburst sampling, an algorithm for automated three-dimensional shape analysis from laser scanning microscopy images. Nature protocols. 2006; 1(4):2152–2161. [PubMed: 17487207]

Rodriguez A, Ehlenberger DB, Hof PR, Wearne SL. Three-dimensional neuron tracing by voxel scooping. J Neurosci Methods. 2009; 184(1):169–175. [PubMed: 19632273]

Sapolsky RM. Do glucocorticoid concentrations rise with age in the rat? Neurobiology of aging. 1992; 13(1):171–174. [PubMed: 1542376]

Seib LM, Wellman CL. Daily injections alter spine density in rat medial prefrontal cortex. Neurosci Lett. 2003; 337(1):29–32. [PubMed: 12524164]

Sesack SR, Deutch AY, Roth RH, Bunney BS. Topographical Organization of the Effect Projections of the Medial Prefrontal Cortex in the Rat: An Anterograde Tract-Tracing Study with Phaseolus

vulgaris Leucoagglutinin. The Journal of comparative neurology. 1989; 290:213–242. [PubMed: 2592611]

Shansky RM, Hamo C, Hof PR, McEwen BS, Morrison JH. Stress-induced dendritic remodeling in the prefrontal cortex is circuit specific. Cerebral cortex. 2009; 19(10):2479–2484. [PubMed: 19193712]

Shors TJ, Weiss C, Thompson RF. Stress-induced facilitation of classical conditioning. Science. 1992; 257(5069):537–539. [PubMed: 1636089]

Sousa N, Lukoyanov NV, Madeira MD, Almeida OF, Paula-Barbosa MM. Reorganization of the morphology of hippocampal neurites and synapses after stress-induced damage correlates with behavioral improvement. Neuroscience. 2000; 97(2):253–266. [PubMed: 10799757]

Swanson AM, Shapiro LP, Whyte AJ, Gourley SL. Glucocorticoid receptor regulation of action selection and prefrontal cortical dendritic spines. Commun Integr Biol. 2013; 6(6):e26068. [PubMed: 24563705]

Tanokashira D, Morita T, Hayashi K, Mayanagi T, Fukumoto K, Kubota Y, Yamashita T, Sobue K. Glucocorticoid suppresses dendritic spine development mediated by down-regulation of caldesmon expression. The Journal of neuroscience: the official journal of the Society for Neuroscience. 2012; 32(42):14583–14591. [PubMed: 23077044]

Tiemensma J, Biermasz NR, Middelkoop HA, van der Mast RC, Romijn JA, Pereira AM. Increased prevalence of psychopathology and maladaptive personality traits after long-term cure of Cushing's disease. J Clin Endocrinol Metab. 2010a; 95(10):E129–141. [PubMed: 20660031]

Tiemensma J, Kokshoorn NE, Biermasz NR, Keijser BJ, Wassenaar MJ, Middelkoop HA, Pereira AM, Romijn JA. Subtle cognitive impairments in patients with long-term cure of Cushing's disease. J Clin Endocrinol Metab. 2010b; 95(6):2699–2714. [PubMed: 20371667]

van Aerde KI, Feldmeyer D. Morphological and physiological characterization of pyramidal neuron subtypes in rat medial prefrontal cortex. Cerebral cortex. 2015; 25(3):788–805. [PubMed: 24108807]

Vertes RP. Differential projections of the infralimbic and prelimbic cortex in the rat. Synapse. 2004; 51(1):32–58. [PubMed: 14579424]

Vogt BA, Peters A. Form and Distribution of Neurons in Rat Cingulate Cortex: Areas 32, 24, and 29. The Journal of comparative neurology. 1981; 195:603–625. [PubMed: 7462444]

Vyas A, Jadhav S, Chattarji S. Prolonged behavioral stress enhances synaptic connectivity in the basolateral amygdala. Neuroscience. 2006; 143(2):387–393. [PubMed: 16962717]

Vyas A, Mitra R, Shankaranarayana Rao BS, Chattarji S. Chronic stress induces contrasating pateterns of dendritic remodeling in hippocampal and amygdaloid neurons. The Journal of neuroscience: the official journal of the Society for Neuroscience. 2002; 22(15):6810–6818. [PubMed: 12151561]

Watanabe Y, Gould E, Cameron HA, Daniels DC, McEwen BS. Phenytoin prevents stress- and corticosterone-induced atrophy of CA3 pyramidal neurons. Hippocampus. 1992a; 2(4):431–435. [PubMed: 1308199]

Watanabe Y, Gould E, McEwen BS. Stress induces atrophy of apical dendrites of hippocampal CA3 pyramidal neurons. Brain research. 1992b; 588(2):341–345. [PubMed: 1393587]

Wellman CL. Dendritic reorganization in pyramidal neurons in medial prefrontal cortex after chronic corticosterone administration. Journal of neurobiology. 2001; 49(3):245–253. [PubMed: 11745662]

Wosiski-Kuhn M, Erion JR, Gomez-Sanchez EP, Gomez-Sanchez CE, Stranahan AM. Glucocorticoid receptor activation impairs hippocampal plasticity by suppressing BDNF expression in obese mice. Psychoneuroendocrinology. 2014; 42:165–177. [PubMed: 24636513]

Yang G, Pan F, Gan WB. Stably maintained dendritic spines are associated with lifelong memories. Nature. 2009; 462(7275):920–924. [PubMed: 19946265]

Yasumatsu N, Matsuzaki M, Miyazaki T, Noguchi J, Kasai H. Principles of long-term dynamics of dendritic spines. The Journal of neuroscience: the official journal of the Society for Neuroscience. 2008; 28(50):13592–13608. [PubMed: 19074033]

Yuen EY, Liu W, Karatsoreos IN, Feng J, McEwen BS, Yan Z. Acute stress enhances glutamatergic transmission in prefrontal cortex and facilitates working memory. Proceedings of the National

Academy of Sciences of the United States of America. 2009; 106(33):14075–14079. [PubMed: 19666502]

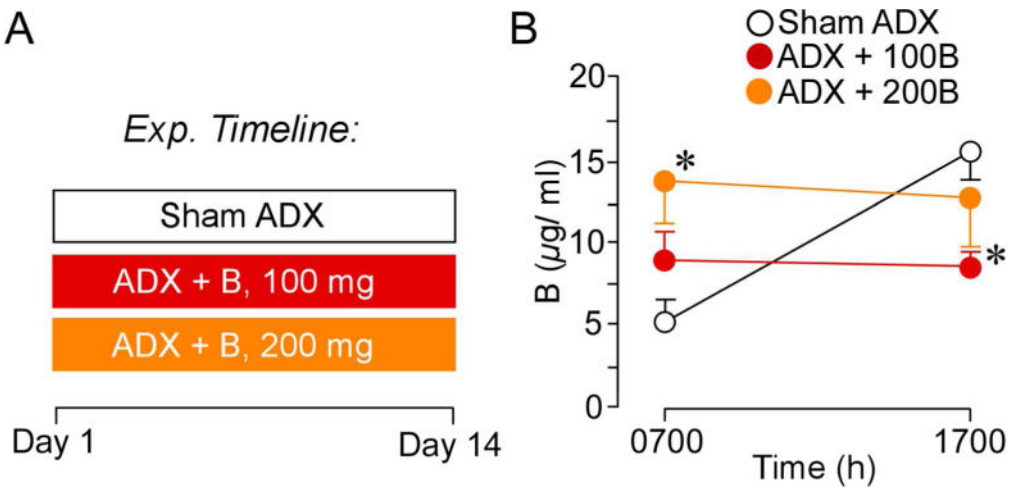

Figure 1.

A. Timeline of the first experiment. On day 1 animals underwent ADX surgeries and B pellet implantation or sham ADX and cholesterol pellet implantation. On day 14 blood was collected to assay for effectiveness of pellet increasing B levels. **B.** Graph depicting mean ± SEM plasma CORT levels at AM and PM sampling of B as a function of treatment group. These data reveal that 200 mg B pellets clamp levels to peak circadian levels, while 100 mg B pellets clamp B levels to values approximating the circadian mean. N = 10, control; N = 6, B100 and B200. *, $p < 0.05$, significantly different from sham-treated animals.

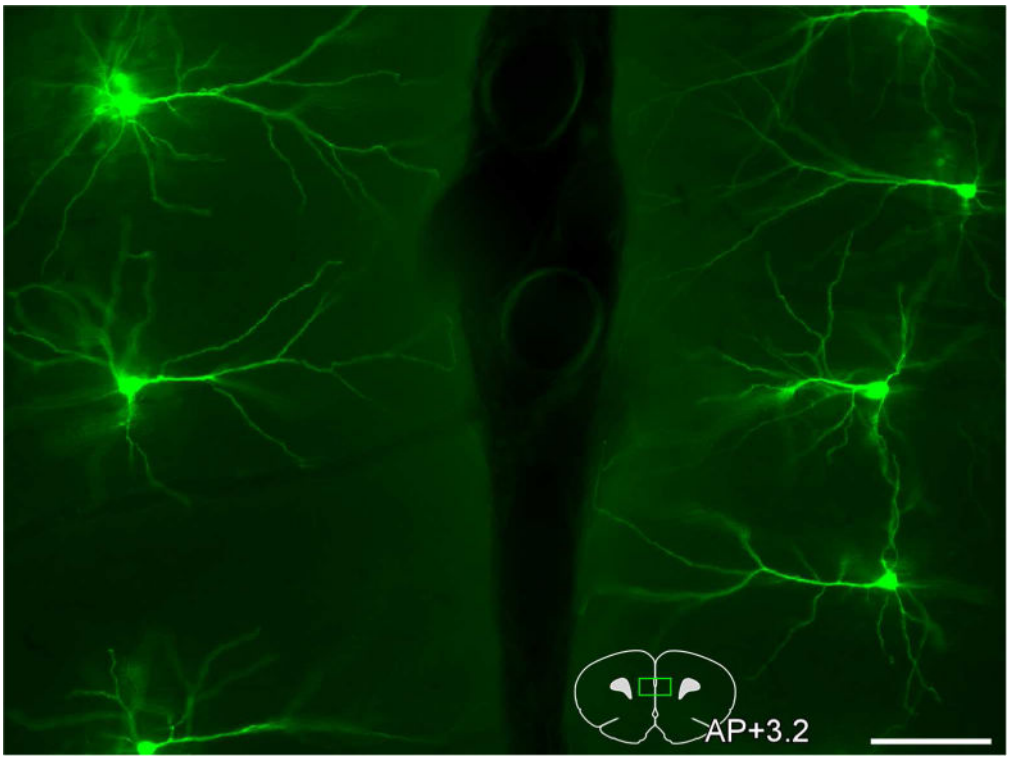

Figure 2.

Darkfield photomicrograph depicting an array of bilateral layer 2 and 3 pyramidal neurons in PL targeted for intracellular dye-injection with Lucifer Yellow (pseudo-colored green). An atlas plate (lower right) depicts the approximate region within PL that neurons were filled for morphologic analyses. Distance in millimeters relative to bregma is indicated. AP, anteroposterior. Scale bar, 100 μm.

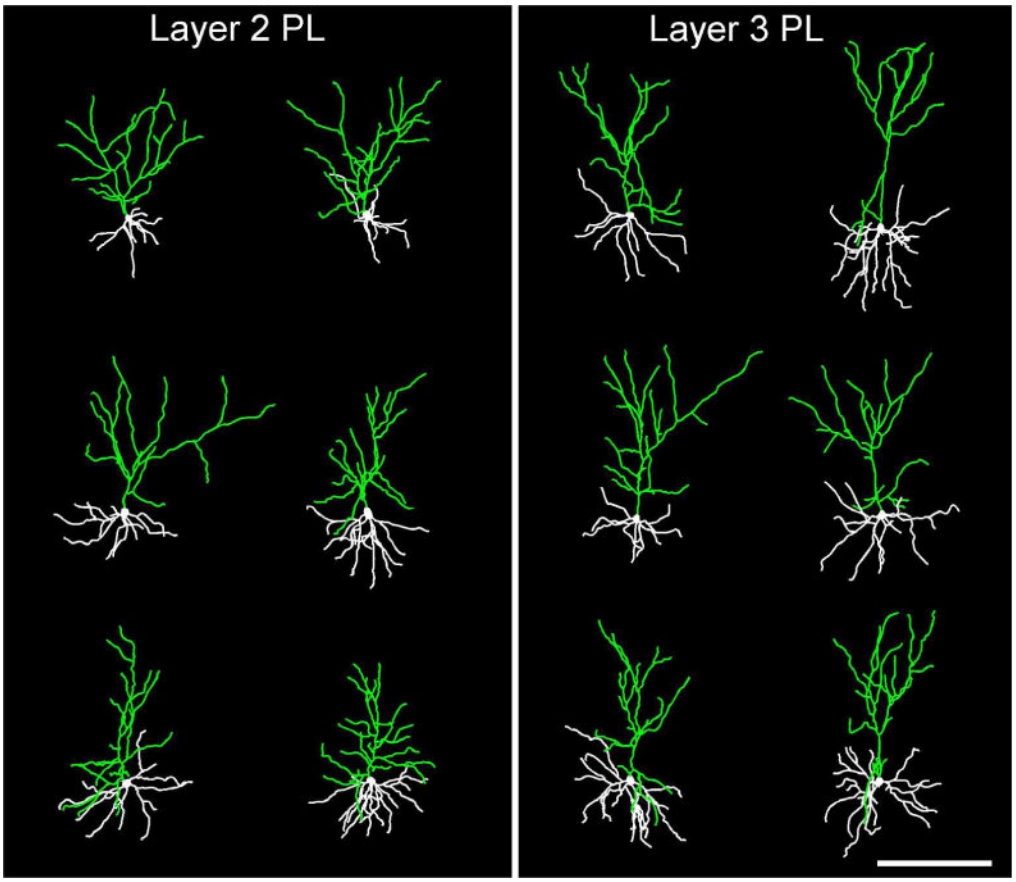

Figure 3.

Examples of 3D digital reconstructions showing Lucifer Yellow-filled layer 2 (left) and layer 3 (right) pyramidal neurons in PL. Contrasting apical dendritic morphologies between these neuronal subtypes are highlighted in green, with layer 3 neurons exhibiting apical dendrites with and initial bifurcation point more distal to the cell body than in layer 2. Scale bar, 200 μm.

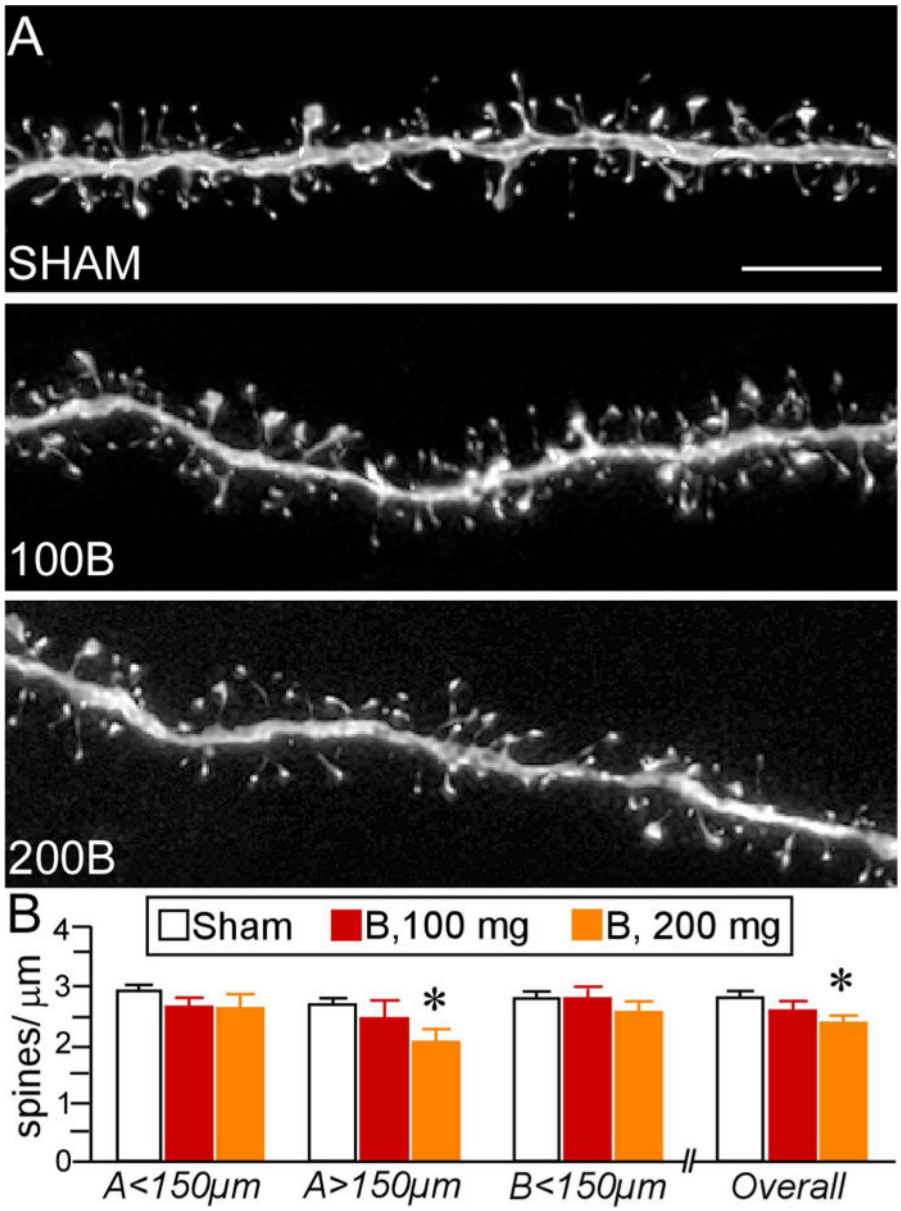

Figure 4.

A. Deconvolved images of dendritic segments from layer 2 and 3 pyramidal neurons in PL from different treatment groups. Scale bar, 5 µm. **B.** Mean + SEM of dendritic spine density as a function of B treatment. B100 animals showed no differences in spine density relative to controls within any region of the dendritic tree. B200 rats displayed overall spine loss, notably in the more distal aspects of the apical tree. N = 10, control; N = 6, B100 and B200. *, $p < 0.05$, significantly different from sham rats.

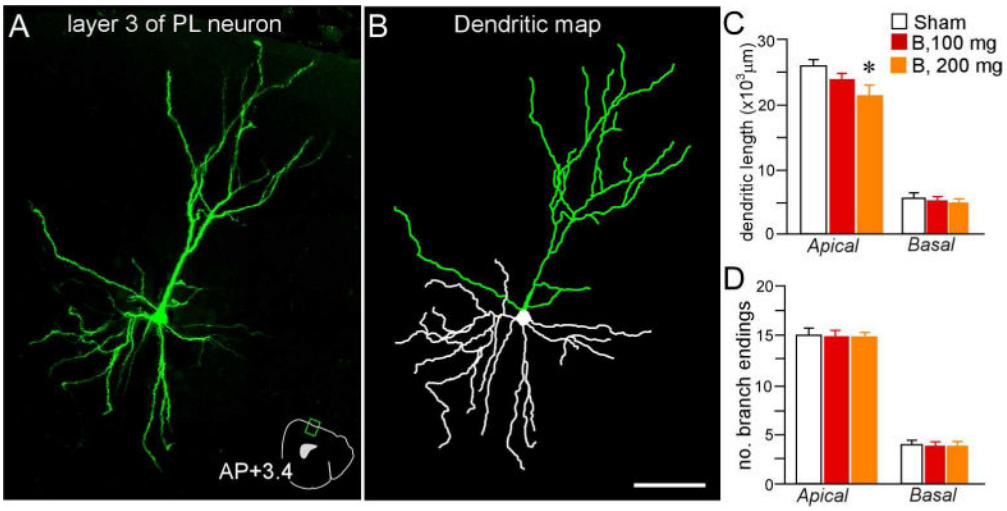

Figure 5.

3D digital reconstruction (**A**) of a Lucifer Yellow-filled layer 2 and 3 PL neuron (pseudocolored green) using confocal laser-scanning microscopy, and the rendering of its dendritic tree (**B**) using computer-assisted morphometry. An atlas plate (**A**, lower right) depicts the neuron's approximate location and angle of orientation within PL. Distance in millimeters relative to bregma is indicated. AP, anteroposterior Scale bar (applies to both), 75 µm. Mean + SEM for dendritic length (**C**) and number of branch endings (**D**) for apical and basal dendrites as a function of treatment group. Only rats that received high-dose glucocorticoids (B, 200 mg) displayed apical dendritic shrinkage. N = 10, control; N = 6, B100 and B200. *, $p < 0.05$, significantly different from sham rats.

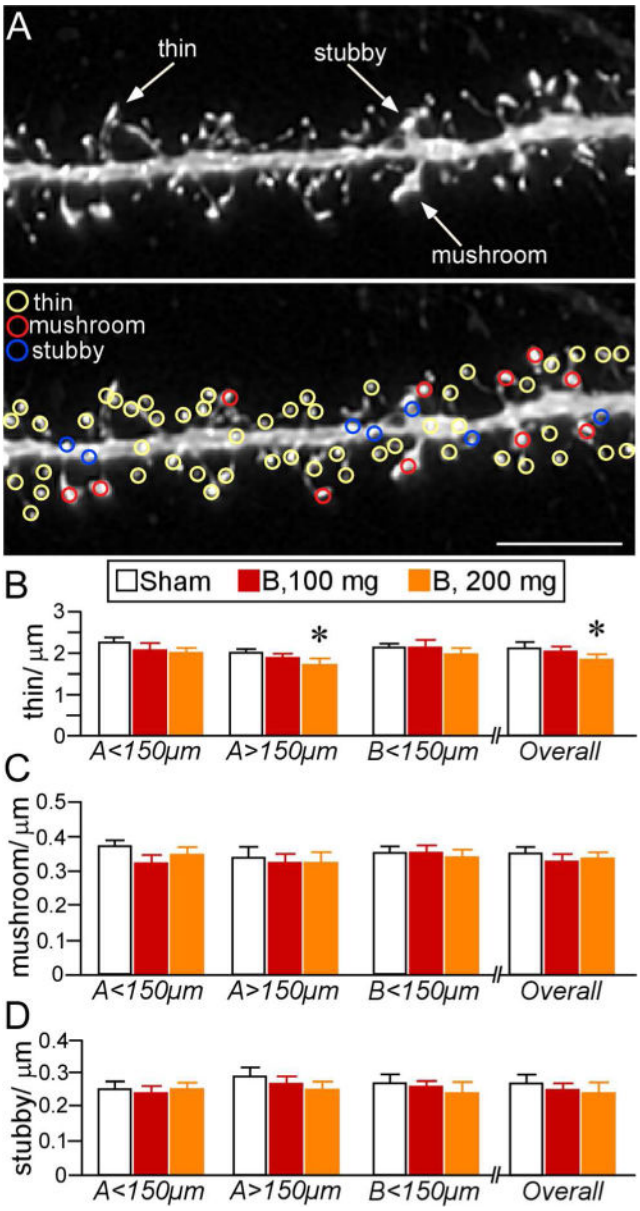

Figure 6.

A. Example of high-resolution deconvolved optical z-stack of a dendritic segment used for spine analysis with NeuronStudio Software. Open colored circles designate spine subtypes based upon user-defined parameters in the software. Scale bar, 5 µm. **B–D.** Mean ± SEM of dendritic spine subtypes. **B.** Thin spine loss was evident in B200 rats, especially at radial distances > 150 µm. No other effects were evident in other subtypes **(C, D).** N = 10, control; N = 6, B100 and B200. *, $p < 0.05$, significantly different from sham rats.

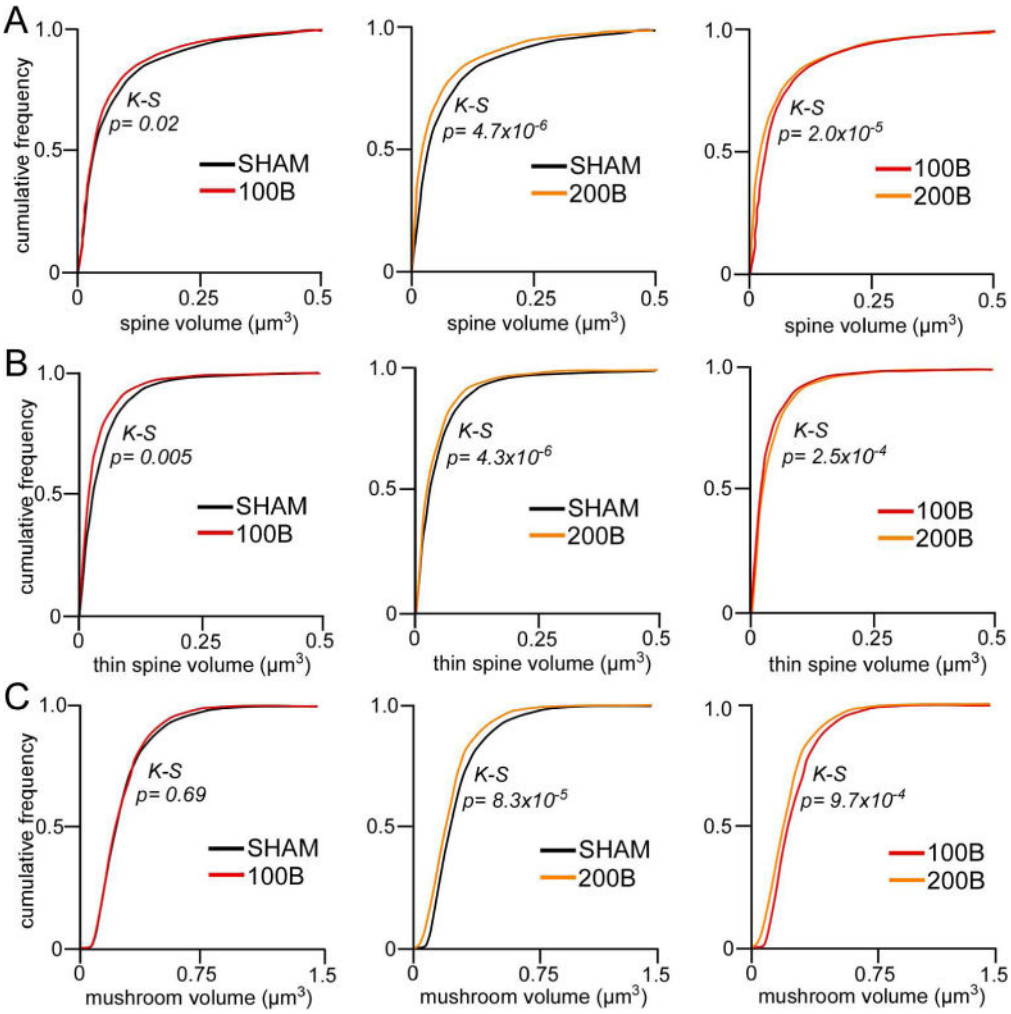

Figure 7.

A. Cumulative frequency distributions of overall spine volume in PL neurons reveal graded leftward shifts (i.e. decrease) in spine volume in B100 and B200 rats, respectively. **B.** This trend is recapitulated in thin spine volumes. **C.** By contrast, B200 rats show selective decreases in mushroom spine volumes relative to B100 and sham groups. K-S, Kolmogrov-Smirnov test, significance set at $p < 0.01$.

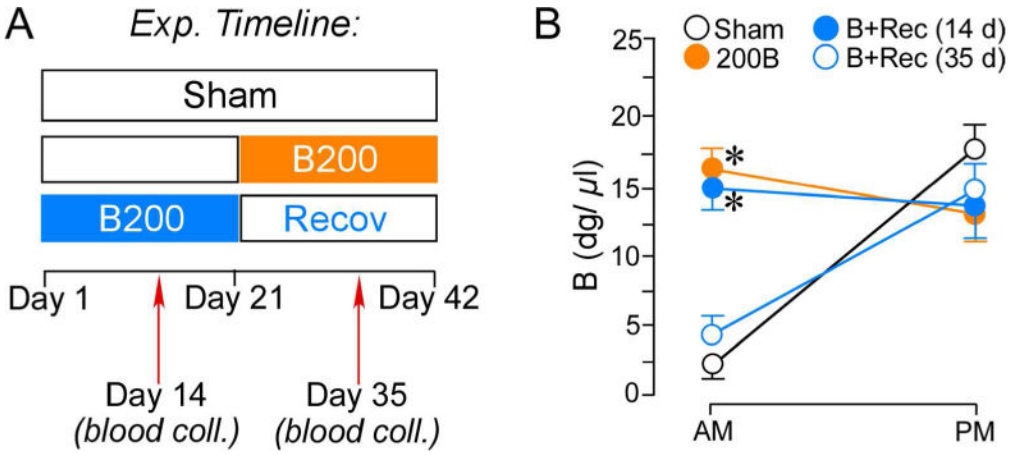

Figure 8.

A. Timeline of the second experiment for high dose B treatment (B200) and comparison with groups of rats given a 3-week recovery period (B + Recov) to restore HPA rhythmicity. On day 14 blood was collected in Sham and B + Recov animals to assay for effectiveness of pellet increasing B in levels. On day 35 blood was collected to assay for effectiveness of pellet increasing B levels in B200 animals and in B + Recov to assay for HPA activity restoration. **B.** B200 and B200 + Recov groups displayed elevated B, and B + Recov rats showed a normalization of adrenocortical function after the cessation of B exposure. N = 6–8 rats per group. *, $p < 0.05$, significantly different from sham group.

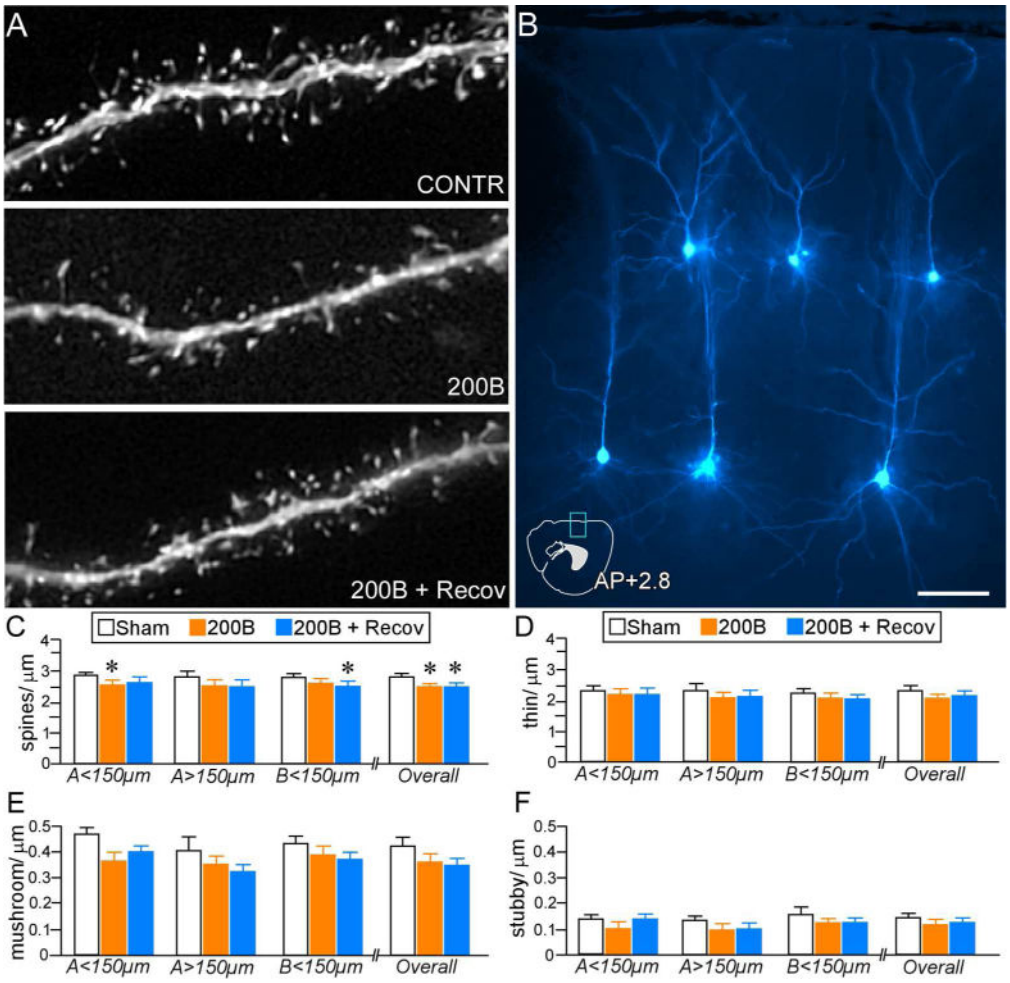

Figure 9.

A. Deconvolved images of dendritic segments from pyramidal neurons in PL from different treatment groups. **B.** Image depicts several layers 2, 3, and 5 dye-filled PL pyramidal neurons (pseudocolored cyan). An atlas plate (lower left) depicts the approximate location and orientation within PL of the dye-filled neurons as shown. Distance in millimeters relative to bregma is indicated. AP, anteroposterior. Scale bar, 5 µm. **C.** Mean + SEM of dendritic spine density and thin subtype density **(D)** as a function of experimental treatment. Both B200 and B200 + Recov groups show overall decreases in density relative to sham rats, whereas only B200 rats show significant reductions in overall thin subtypes. **E.** Mean + SEM of mushroom and stubby **(F)** spine densities in treatment groups. Both 200B and 200B + Recov groups display evidence of mushroom spine loss at various regions of the dendritic tree, whereas B200 + Recov rats display overall decreases, relative to sham control rats. N = 6–8 rats per group *, $p < 0.05$, significantly different relative to sham group.

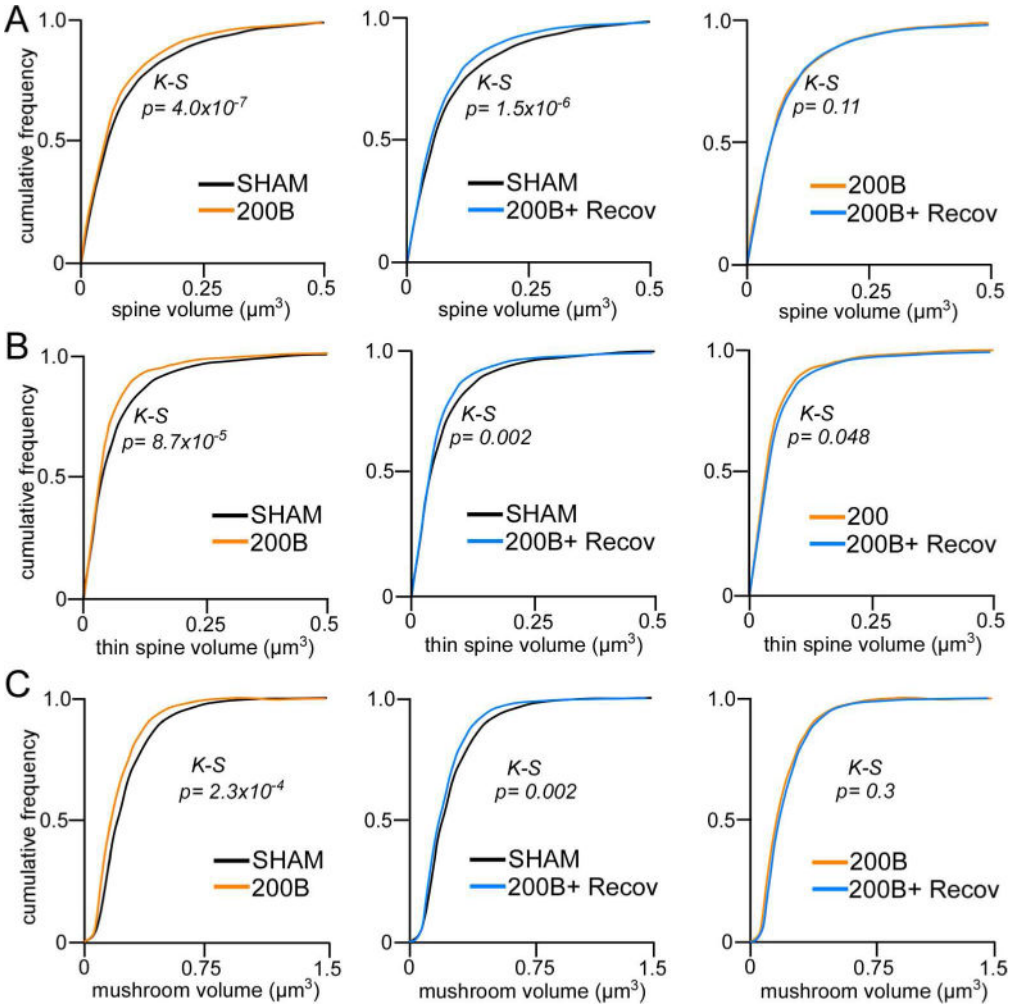

Figure 10.

A. Cumulative frequency distributions of overall spine volume in PL neurons reveal leftward shifts (i.e. decrease) in spine volume following B200 treatment, even after a 21-day recovery period. This trend is also evident in thin (**B**) and mushroom (**C**) subtypes with respect to sham control rats. K-S, Kolmogrov-Smirnov test, significance set at $p < 0.01$.

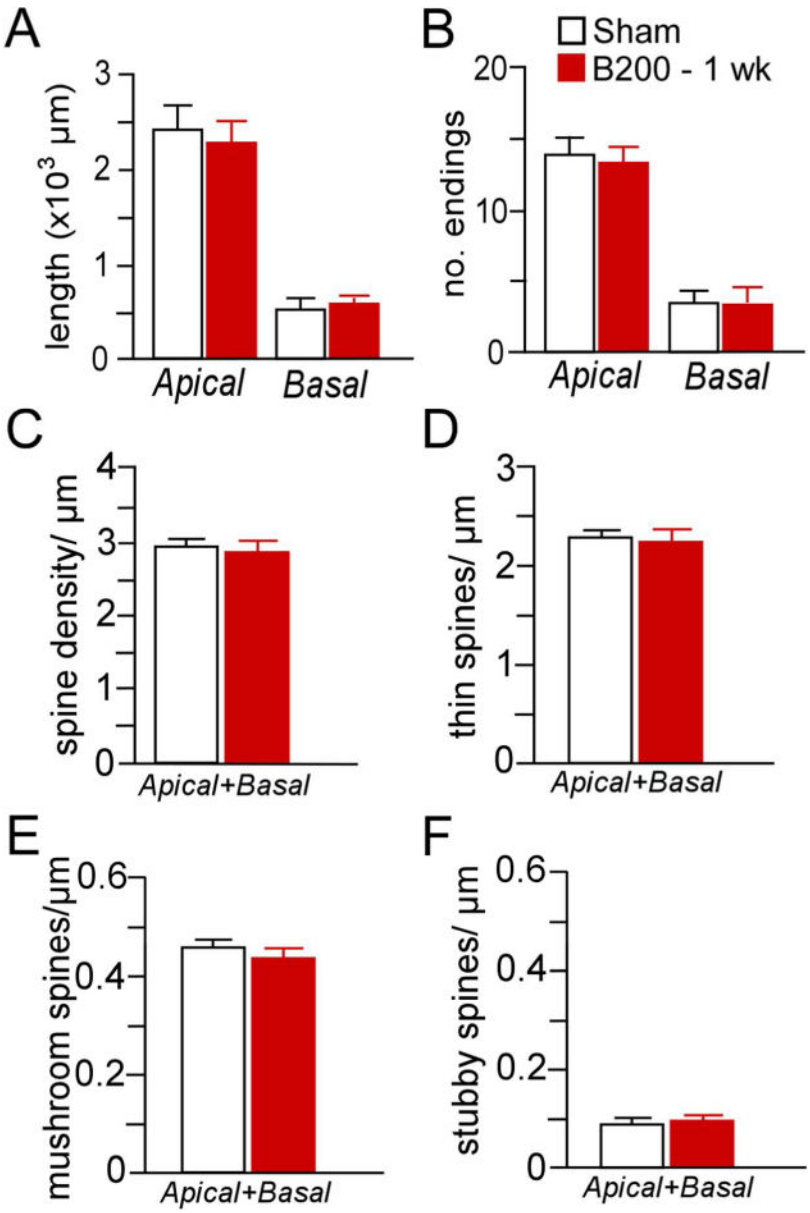

Figure 11.

Mean + SEM for dendritic length (***A***) and number of branch endings (**B**) after 1 week of exposure to high-dose B (200 mg pellet, s.c.). Mean + SEM for overall (**C**), thin (**D**), mushroom (**E**), and stubby (**F**) spine densities as a function of B200 or sham pellets. This duration of glucocorticoid exposure failed to induce any frank differences in the dendritic or spine morphologic indices examined in PL neurons. N = 5–6 rats per group.

Table 1

Data Summary for Experiment 1 - Effects of varying doses of B on structural plasticity in PL

Treatment	Sham	100B	200B
Animals	10	6	6
Neurons	66	36	36
Neurons/animal	6–7	6	6
Laminae Analyzed	Layers 2 and 3	Layers 2 and 3	Layers 2 and 3
Spines	27,225	14,458	12,554
Overall Spine Density ± SEM	2.75 ± 0.06	2.63 ± 0.17	2.47 ± 0.12*
Thin Spine Density ± SEM	2.13 ± 0.06	2.03 ± 0.15	1.89 ± 0.12*
Mushroom Spine Density ± SEM	0.35 ± 0.02	0.34 ± 0.02	0.33 ± 0.02
Stubby Spine Density ± SEM	0.27 ± 0.02	0.25 ± 0.01	0.25 ± 0.01
Neurons/animal – dendritic arborization analysis	5–6**	4–5**	4–6**
Apical dendrite length	2819 ± 135	2467 ± 255	2164 ± 214*
Apical branch endings	15 ± 1.1	14 ± 1.2	14 ± 0.7
Basal dendrite length	617.8 ± 45	568.4 ± 56	519.8 ± 50
Basal branch endings	4.9 ± 0.46	4.5 ± 0.38	4.46 ± 0.38

* Indicates significant difference ($p < 0.05$) when compared to control treatment group.

** Due to strict inclusion criteria (see Methods), the number of neurons analyzed in the dendritic arborization analysis is smaller than the number of neurons analyzed in the dendritic spine analysis.

Table 2

Data summary for Experiment 2 - Persistence of B-induced structural alterations in PL following a 3-week recovery period

Treatment	**Sham**	**200B**	**200B + Recovery**
Animals	6	7	8
Neurons	40	53	60
Neurons/animal	6–7	7–8	7–8
Laminae Analyzed	Layers 2, 3, and 5	Layers 2, 3, and 5	Layers 2, 3, and 5
Spines	17,400	20,800	23,400
Overall Spine Density ± SEM	2.87 ± 0.07	2.62 ± 0.08 *	2.61± 0.08 *
Thin Spine Density ± SEM	2.31 ± 0.07	2.12 ± 0.07	2.11 ± 0.07
Mushroom Spine Density ± SEM	0.43 ± 0.01	0.4 ± 0.02	0.38 ± 0.02
Stubby Spine Density ± SEM	0.13 ± 0.01	0.11 ± 0.01	0.12 ± 0.01
Neurons/animal – dendritic arborization analysis	N/A	N/A	N/A
Apical dendrite length	N/A	N/A	N/A
Apical branch endings	N/A	N/A	N/A
Basal dendrite length	N/A	N/A	N/A
Basal branch endings	N/A	N/A	N/A

* Indicates significant difference ($p < 0.05$) when compared to control treatment group.

Table 3

Data summary for Experiment 3 - Effects of short-term B exposure on structural plasticity in PL

Treatment	Sham	200B – 1 week
Animals	6	5
Neurons	34	26
Neurons/animal	5–6	5–6
Laminae Analyzed	Layers 2 and 3	Layers 2 and 3
Spines	13,095	10,763
Overall Spine Density ± SEM	2.91 ± 0.13	2.87 ± 0.10
Thin Spine Density ± SEM	2.37 ± 0.11	2.35 ± 0.07
Mushroom Spine Density ± SEM	0.45 ± 0.02	0.42 ± 0.03
Stubby Spine Density ± SEM	0.09 ± 0.01	0.10 ± 0.01
Neurons/animal – dendritic arborization analysis	4–5 **	4–5 **
Apical dendrite length	1814 ± 261	1679 ± 167
Apical branch endings	12 ± 1.5	11 ± 1.1
Basal dendrite length	329 ± 38	340 ± 30
Basal branch endings	2.8 ± 0.22	2.9 ± 0.17

* Indicates significant difference ($p < 0.05$) when compared to control treatment group.

** Due to strict inclusion criteria, the number of neurons analyzed in the dendritic arborization analysis is smaller than the number of neurons analyzed in the dendritic spine analysis.